2. Bandstructure of monolayer graphene

Why graphene ?

graphene is **2D**, “relativistic”, chiral and won a flagship !

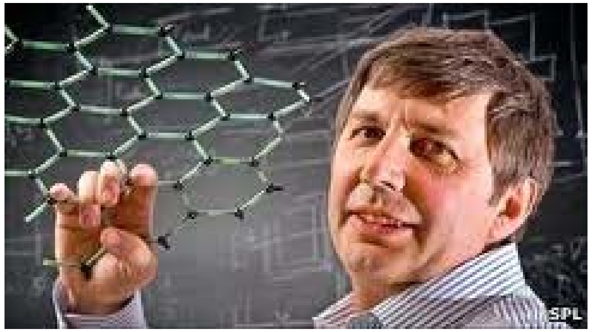

GRAPHENE FLAGSHIP

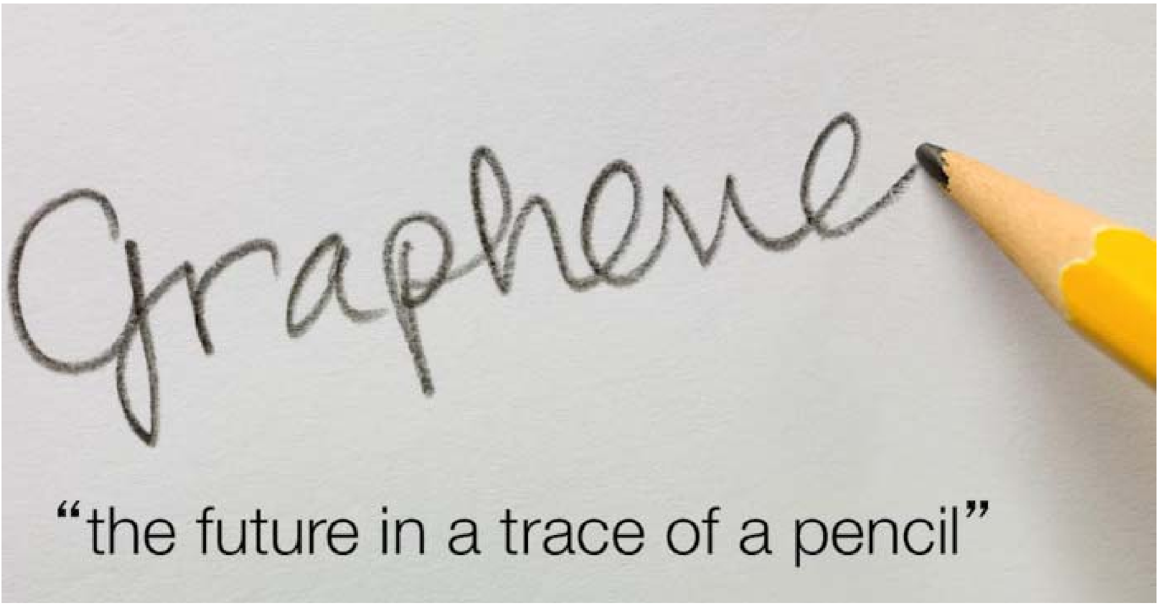

- thin, but strong
- best thermal conductor
- excellent electrical conductor
- transparent
- flat 2.3% light absorption
- applications …

Graphene is 2D

dimensional dependence of electronic properties

when do **metals** exists ?

0d “insulator”

1d (infinite long wire) insulator for T→0

2d **?**

3d there are materials that stay metals at all temperatures

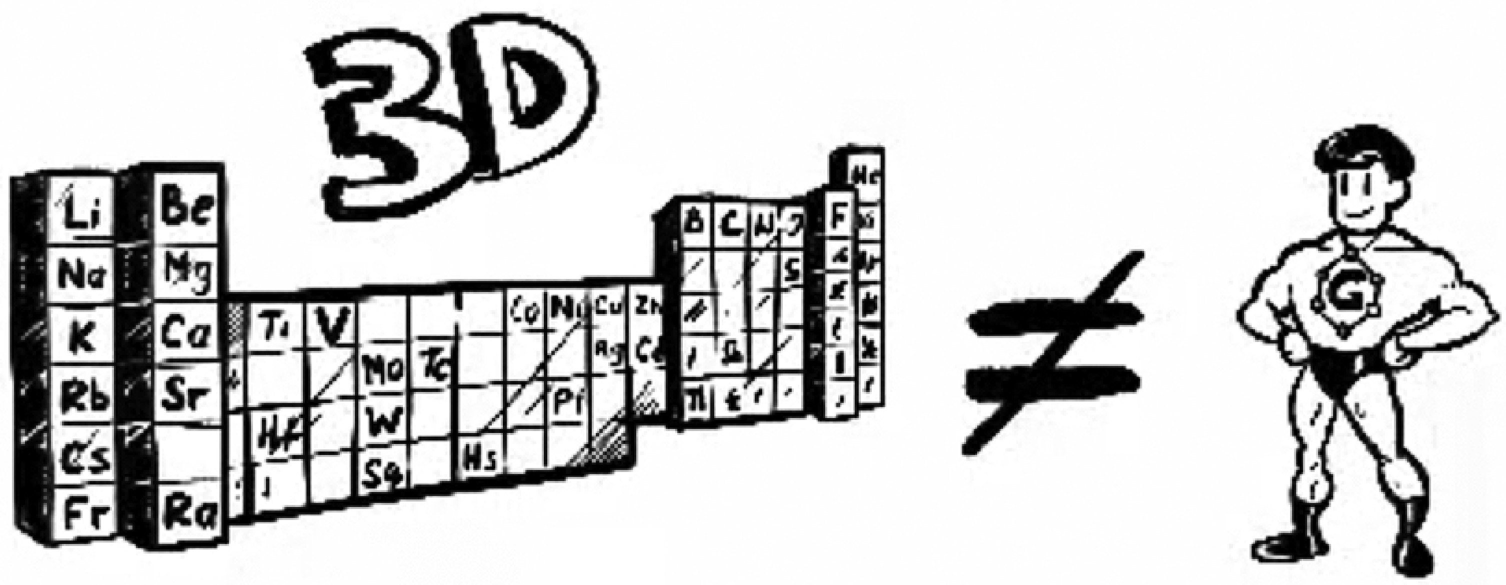

Graphene

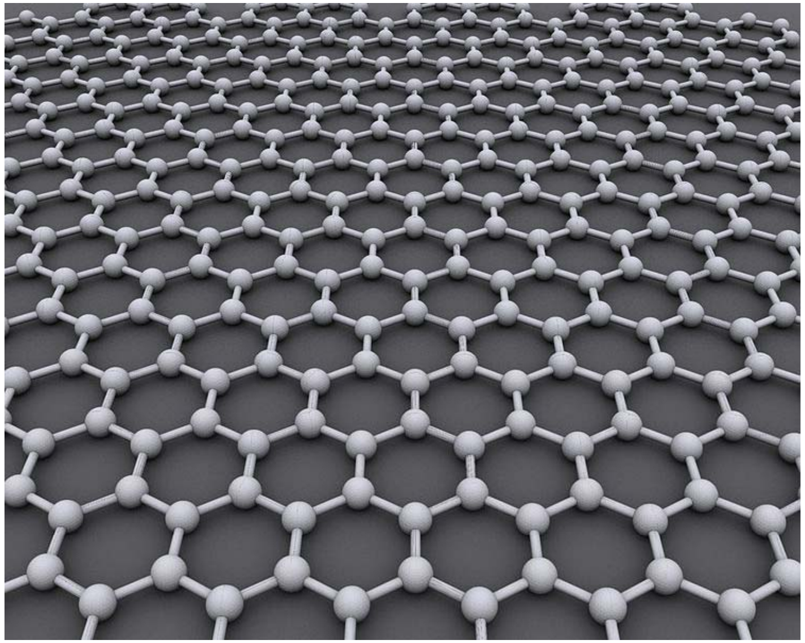

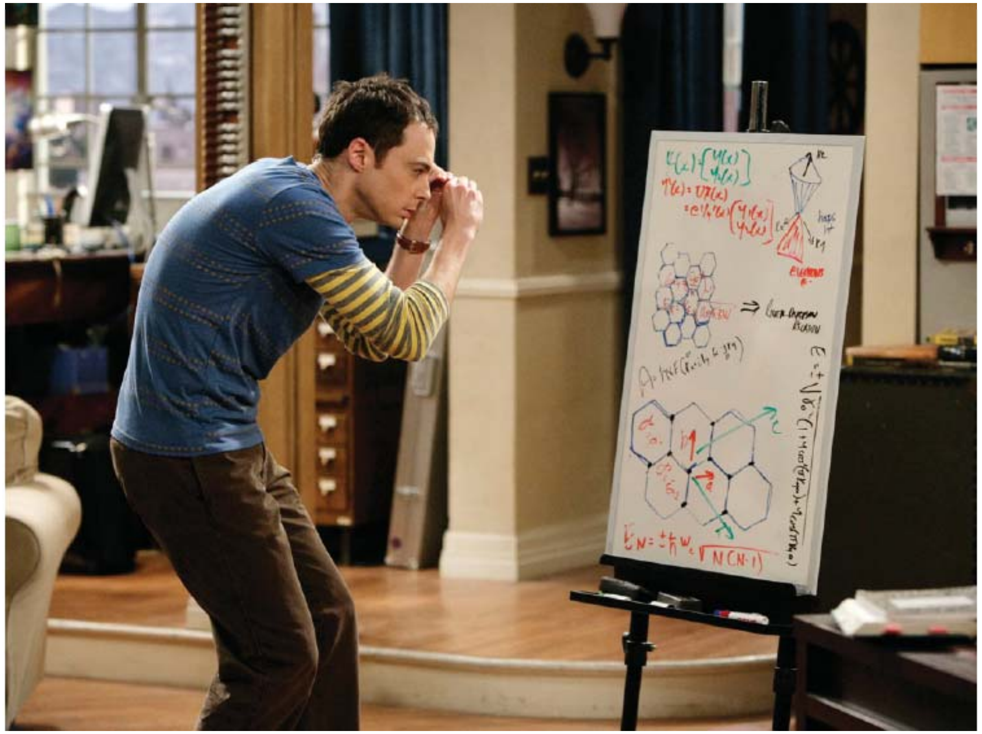

Sheldon in
Big Bang Theory

Bandstructure of graphene

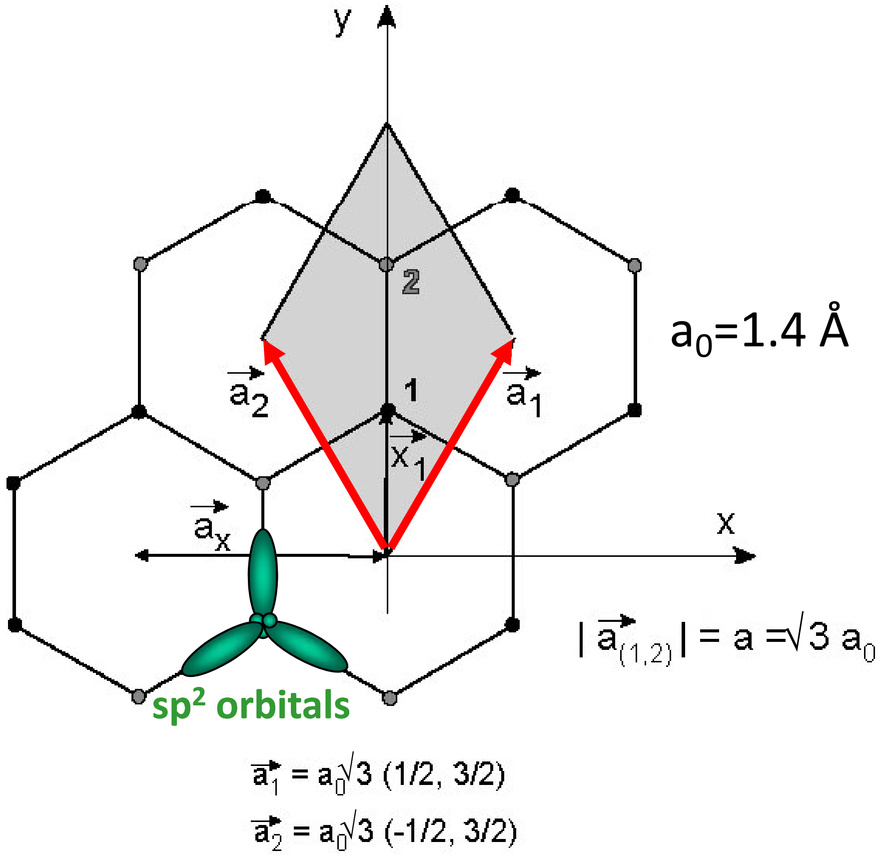

I follow the manuscript "Bandstructure of Graphene and Carbon Nanotubes: An Exercise in Condensed Matter Physics". I abbreviate this with BG

$3 \cdot sp^2$ orbitals/bonding,
4th valence electron ⇨
„bonding" and „antibonding" states

π and π^* bands

Bandstructure of graphene

I follow the manuscript "Bandstructure of Graphene and Carbon Nanotubes: An Exercise in Condensed Matter Physics". I abbreviate this with BG

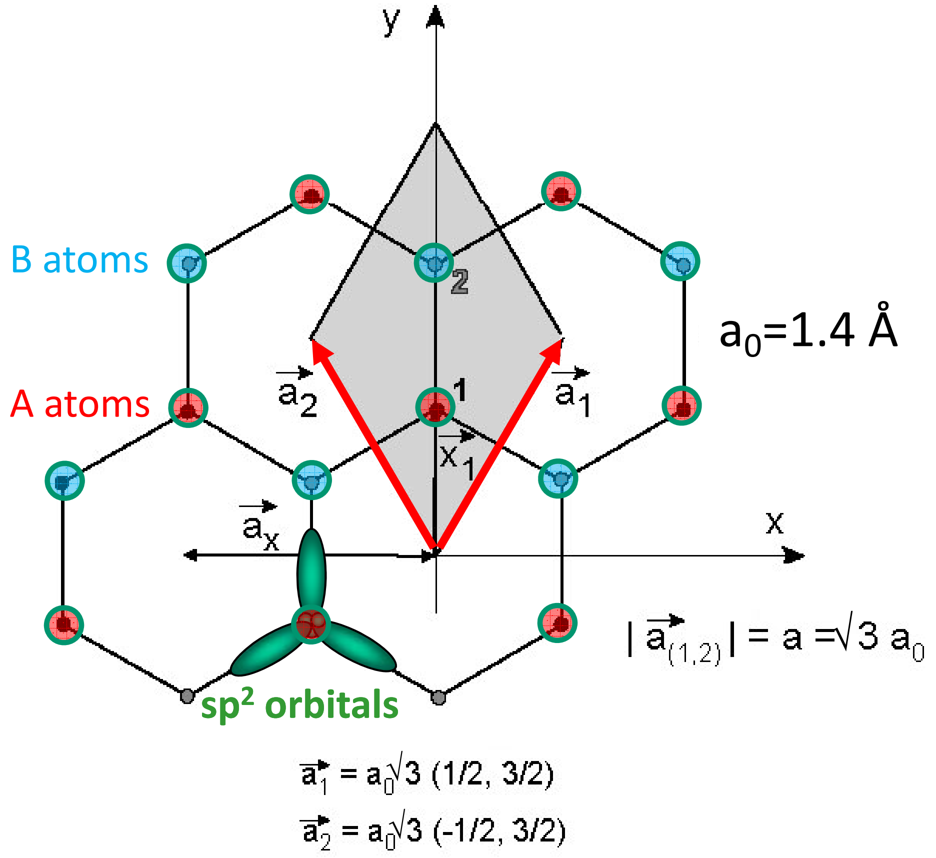

3 · sp^2 orbitals/bonding,
4th valence electron ⇨
„bonding" and „antibonding" states

π and π* bands

goal: calculate the energy of the eigenstates in tight-binding approximation (LCAO). Further, derive a simplified (effective) Hamiltonian.

Bandstructure of graphene, see BG-2 to 15

Ansatz of the wavefunction (Bloch function)

$$\psi_{\vec{k}} = \sum_{\vec{R}\in G} e^{i\vec{k}\cdot\vec{R}}\phi(\vec{x}-\vec{R}) \, ,$$

R is a lattice vector and ϕ_1, ϕ_2 are p_z orbitals of the A(1) and B(2) sites

$$\phi(\vec{x}) = b_1\phi_1(\vec{x}) + b_2\phi_2(\vec{x}) = \sum_n b_n\phi_n$$

Hamiltonian:

$$H = \frac{\vec{p}^2}{2m} + \sum_{\vec{R}\in G}\left(V_{at}(\vec{x}-\vec{x}_1-\vec{R}) + V_{at}(\vec{x}-\vec{x}_2-\vec{R})\right)$$

Note: in this problem there are only two unknowns, b_1 and b_2. Hence 2 equations need to be derived. These can be obtained by using expectation values of the Schrödinger equation:

$$H\psi_k = E(k)\psi_k \quad \begin{cases} \langle\phi_1|H|\psi_k\rangle = E\langle\phi_1|\psi_k\rangle \longrightarrow \langle\phi_1|\Delta U|\psi_k\rangle \cong Eb_1 \longrightarrow \gamma_1\alpha\cdot b_2 \cong Eb_1 \\ \langle\phi_2|H|\psi_k\rangle = E\langle\phi_2|\psi_k\rangle \longrightarrow \langle\phi_2|\Delta U|\psi_k\rangle \cong Eb_2 \longrightarrow \gamma_1\alpha^*\cdot b_1 \cong Eb_2 \end{cases}$$

where $\gamma_1 = \langle\phi_1|\Delta U|\phi_2\rangle$ is the nearest neighbor overlap, which has three contributions captured by α

$$\alpha(\vec{k}) = 1 + e^{-i\vec{k}\cdot\vec{a}_1} + e^{-i\vec{k}\cdot\vec{a}_2}$$

$$\boxed{\gamma_1\begin{pmatrix} 0 & \alpha \\ \alpha^* & \end{pmatrix}\begin{pmatrix} b_1 \\ b_2 \end{pmatrix} = E\begin{pmatrix} b_1 \\ b_2 \end{pmatrix}}$$

note: this is already a bit more simplified than equation BG-15
(a further assumption is that the energy of the atomic p_z orbital is set to zero)

Bandstructure of graphene

$$\boxed{\gamma_1\begin{pmatrix} 0 & \alpha \\ \alpha^* & \end{pmatrix}\begin{pmatrix} b_1 \\ b_2 \end{pmatrix} = E\begin{pmatrix} b_1 \\ b_2 \end{pmatrix}} \Rightarrow E(\vec{k}) = \pm\gamma_1\left|\alpha(\vec{k})\right|$$

$$E(k_x,k_y) = \pm\gamma_1\sqrt{1+4cos\left(\frac{\sqrt{3}ak_y}{2}\right)cos\left(\frac{ak_x}{2}\right)+4cos^2\left(\frac{ak_x}{2}\right)} \qquad (18)$$

a is the lattice constant, i.e. $a=\sqrt{3}a_0$. Note: Tero's a is my a_0

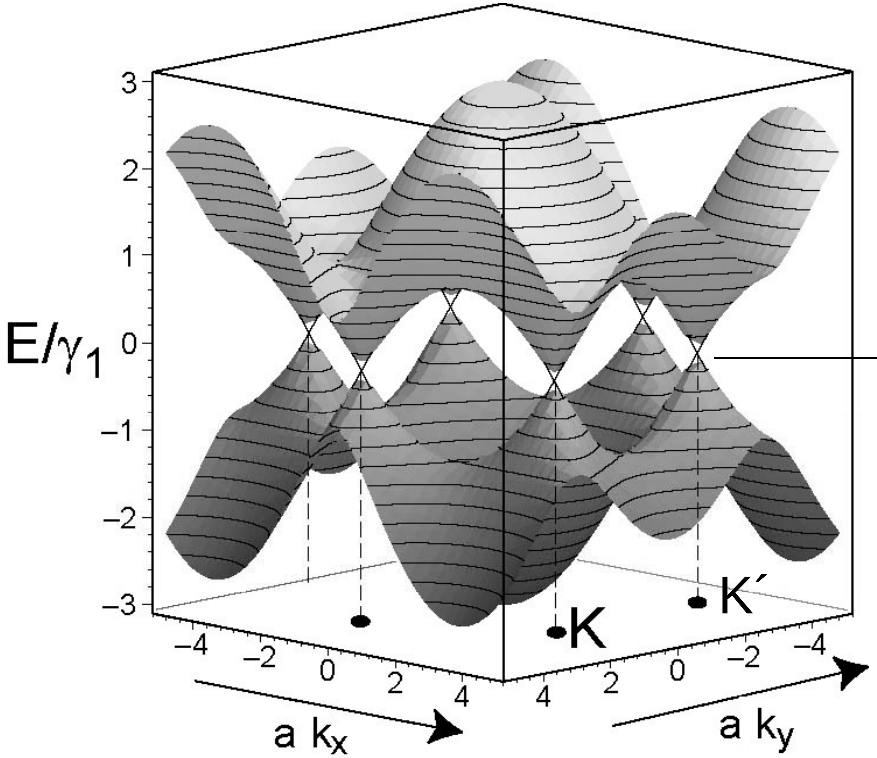

π* antibonding

Fermi energy E_F

π bonding

reciprocal lattice

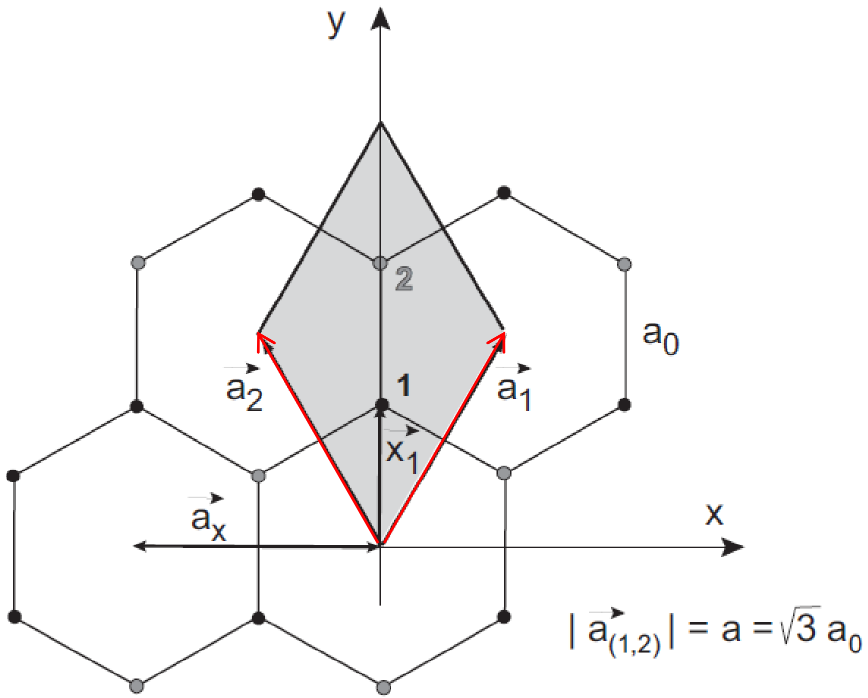

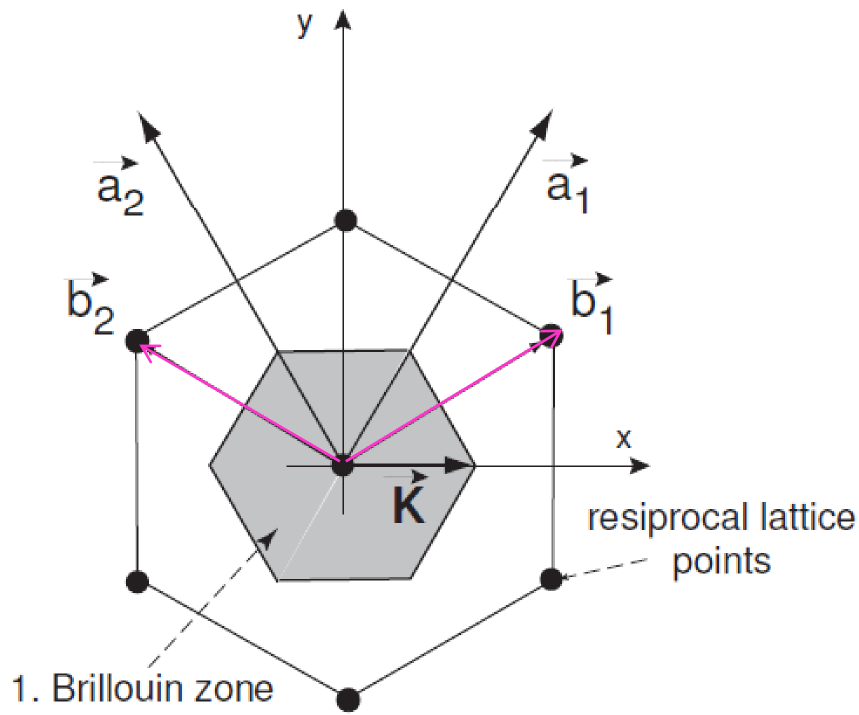

Bandstructure of graphene

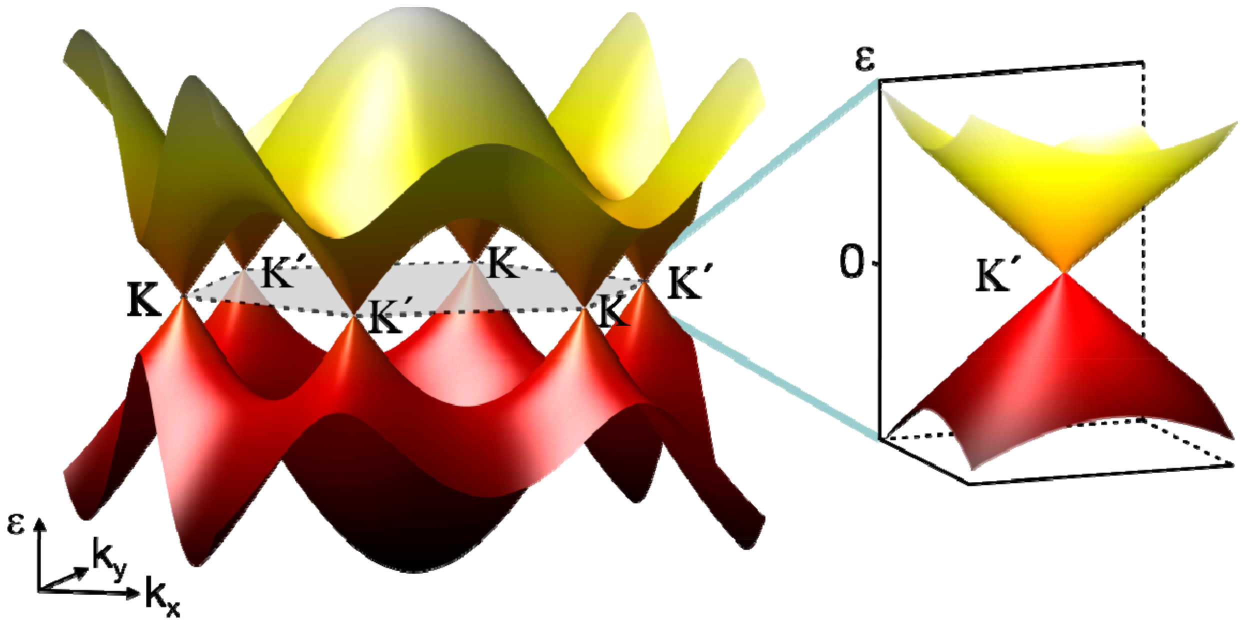

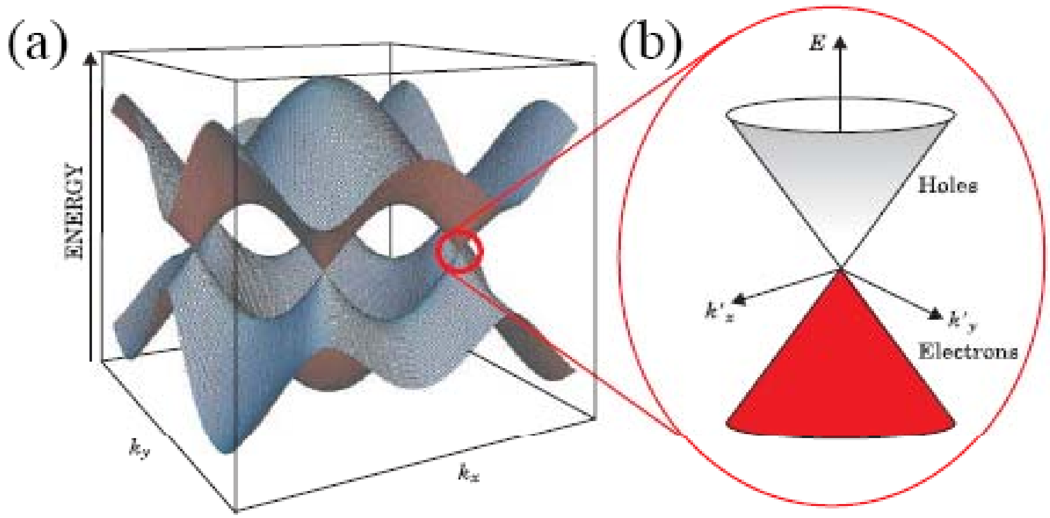

Bandstructure of graphene

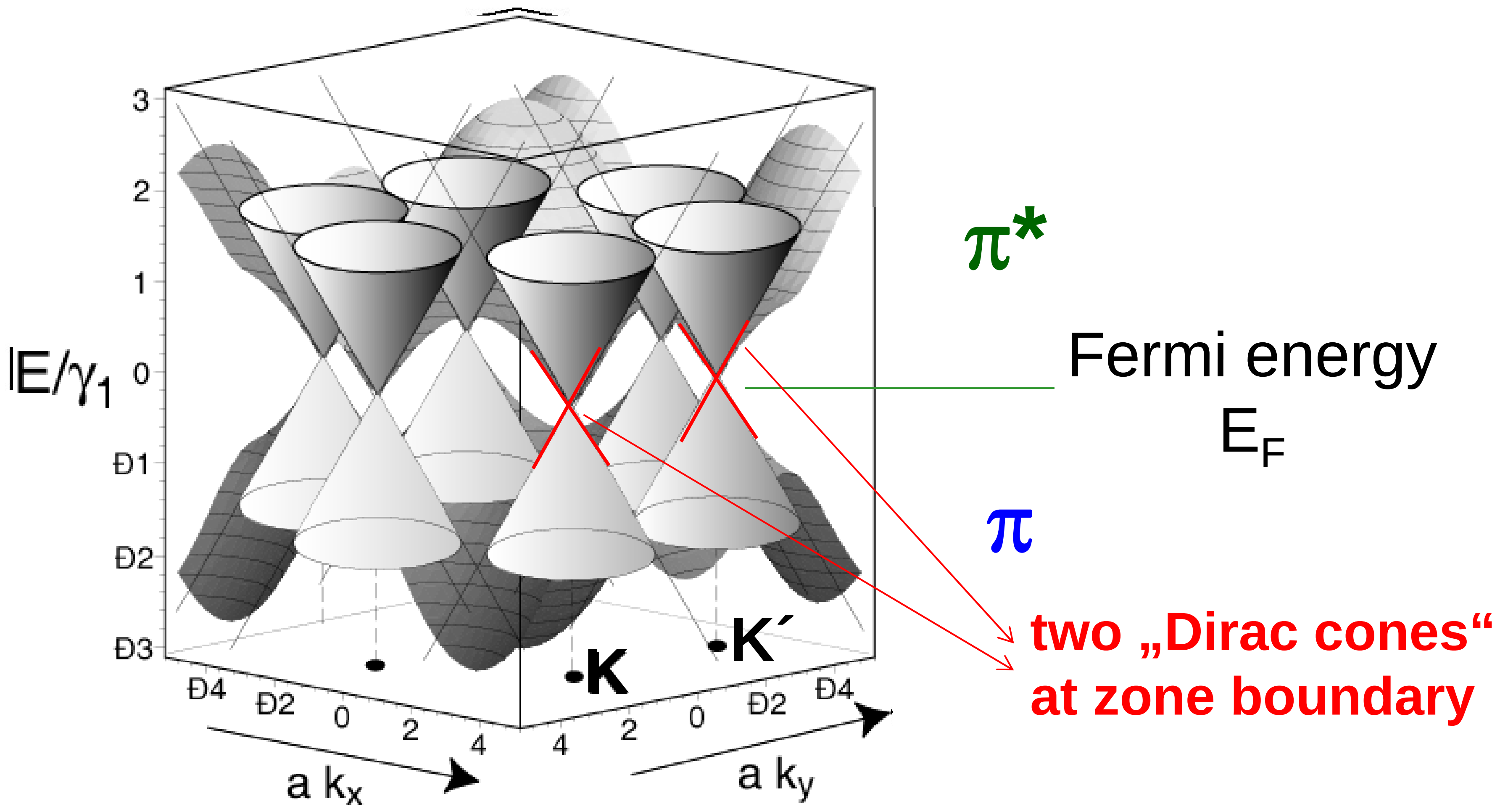

Bandstructure of graphene

$$\boxed{\gamma_1 \begin{pmatrix} 0 & \alpha \\ \alpha^* & \end{pmatrix} \begin{pmatrix} b_1 \\ b_2 \end{pmatrix} = E \begin{pmatrix} b_1 \\ b_2 \end{pmatrix}}$$

dispersion relation

$$\boxed{\varepsilon(\vec{\kappa}) = \pm \hbar v_F \left| \vec{\kappa} \right|}$$

linearize around e.g. K-point: $\vec{k} = \vec{K} + \vec{\kappa}$

$$\varepsilon(\vec{\kappa}) = E(\vec{k}) - E(\vec{K})$$

(note, one gets in addition an expression forthe Fermi velocity)

$$\tilde{H} = \hbar v_F \begin{pmatrix} 0 & \mp\kappa_x - i\kappa_y \\ \mp\kappa_x + i\kappa_y & 0 \end{pmatrix} = \hbar v_F \left(\mp \kappa_x \sigma_x + \kappa_y \sigma_y \right)$$

The two signs correspond to **the two valleys**, see Heikkilä equ. (10.10)
Note: the **Pauli matrices** operate on **"pseudo-spin"** (b1,b2). The real spin is conserved in the Hamiltonian.
Note further that for one sign the equation is exactly the **massless Dirac equation** in 2D

$$H_D = c\vec{\sigma} \cdot \vec{p} + \beta mc^2$$

the velocity of light c is replaced by v_F

Bandstructure of graphene

$$\begin{pmatrix} \mu_g & \hbar v_F\left(\pm i\frac{\partial}{\partial x}+\frac{\partial}{\partial y}\right) \\ \hbar v_F\left(\pm i\frac{\partial}{\partial x}-\frac{\partial}{\partial y}\right) & \mu_g \end{pmatrix}\begin{pmatrix}\psi_A(x,y)\\ \psi_B(x,y)\end{pmatrix} = E\begin{pmatrix}\psi_A(x,y)\\ \psi_B(x,y)\end{pmatrix} \tag{10.11}$$

$$\Psi(x,y)=\frac{1}{\sqrt{2}}\begin{pmatrix}e^{\mp i\phi/2}\\ se^{\pm i\phi/2}\end{pmatrix}e^{i(\pm k_x x+k_y y)}$$

$$E(\vec{k})=\mu_g\pm\hbar v_F\left|\vec{k}\right|$$

+/- corresponds to the two valleys

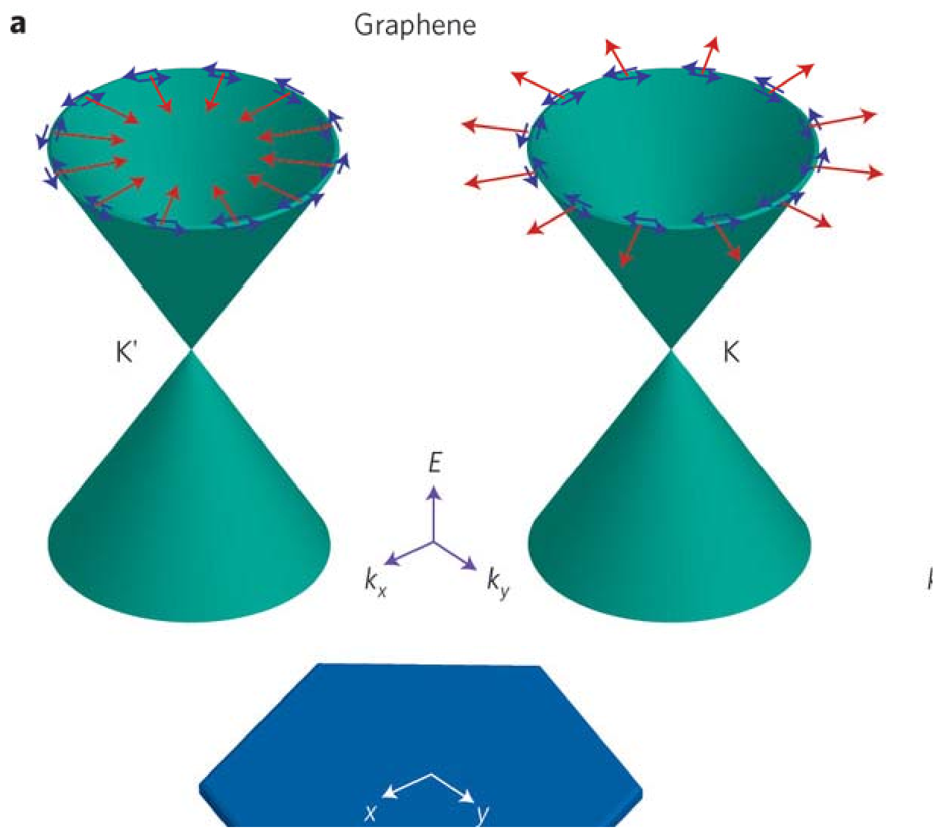

Note: Tero uses again E and k. Also s=sign(E) further:

$$\phi=\arctan(k_x/k_y)$$

pseudospin is linked to momentum
➔ **graphene is chiral**

Chirality in graphene (and CNT)

one can define a helicity as: $\vec{h} = \frac{1}{2}\vec{\sigma} \cdot \frac{\vec{k}}{|\vec{k}|}$

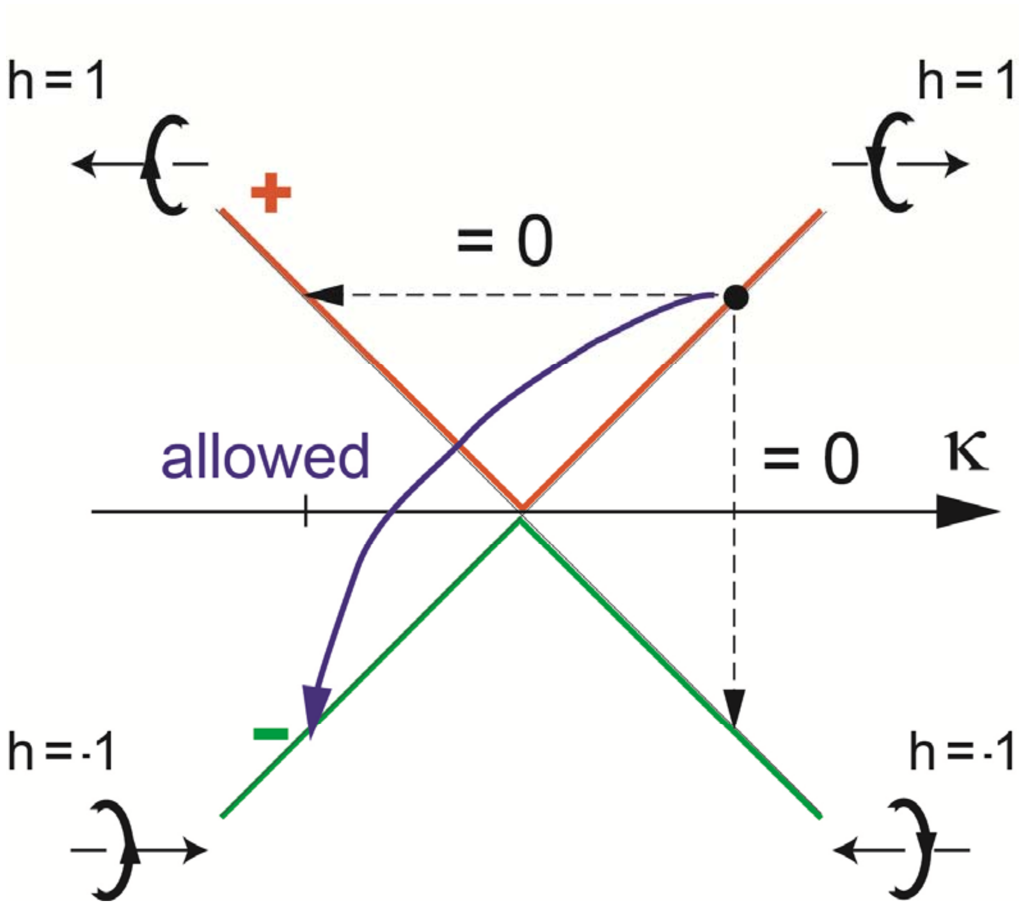

Paul Mc Euen et al. Phys. Rev. Lett. 83, p5098 (1999)

3. Bandstructure of carbon nanotubes and graphene nanoribbons

Bandstructure of carbon nanotubes

chiral vector $\vec{w} = n_1\vec{a}_1 + n_2\vec{a}_2$

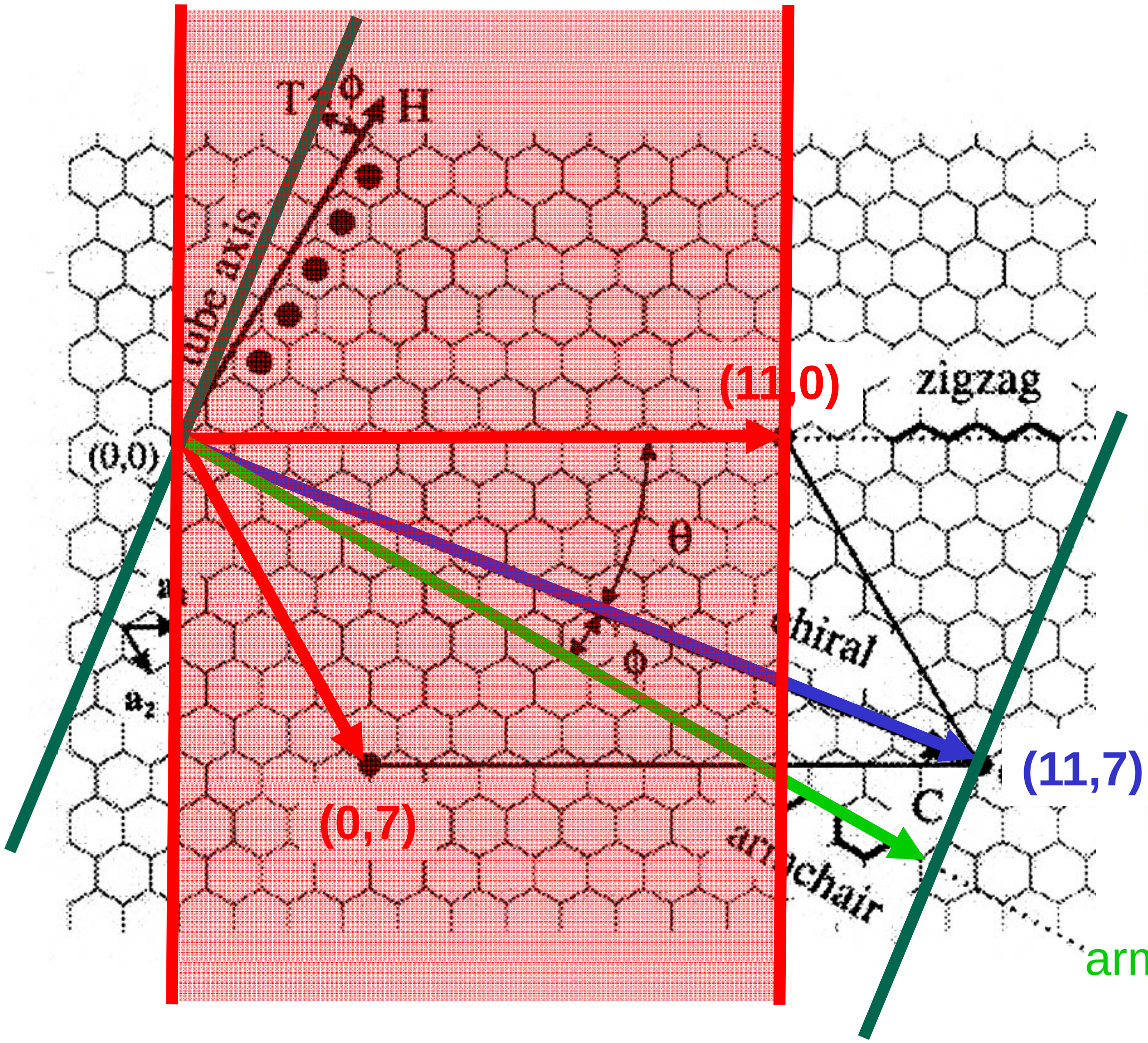

armchair (n,n)=(9,9)

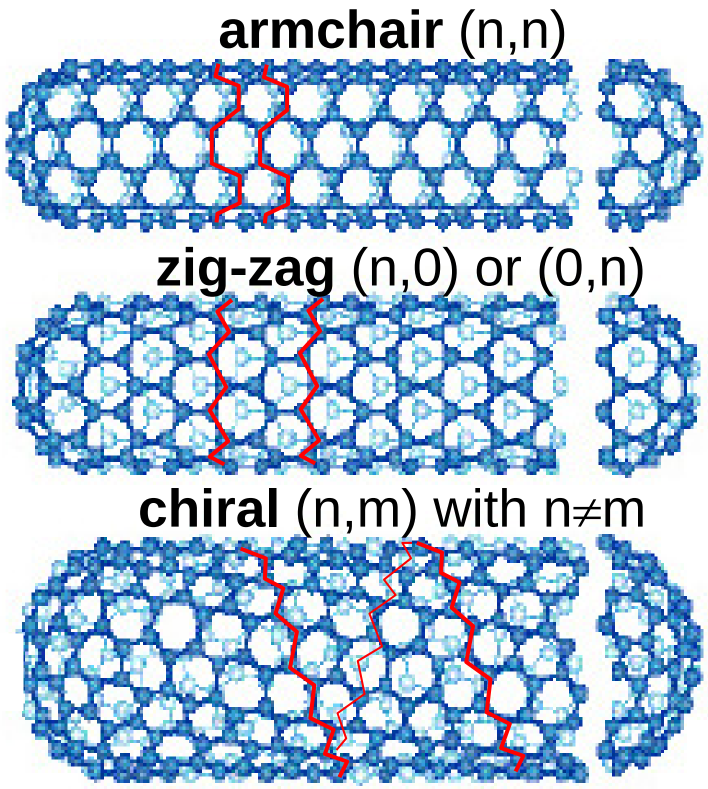

example: armchair CNT

$$\vec{w} = n_1\vec{a}_1 + n_2\vec{a}_2$$

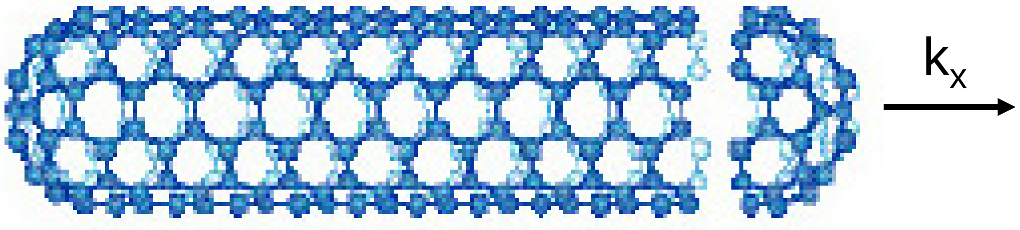

from note CS: example (10,10) armchair tube

k_x is continuous, but...
k_y is discrete due to periodic boundary conditions:

$$k_y = 2\pi\frac{m}{|\vec{w}|} = \frac{m2\pi}{N\sqrt{3}a}$$

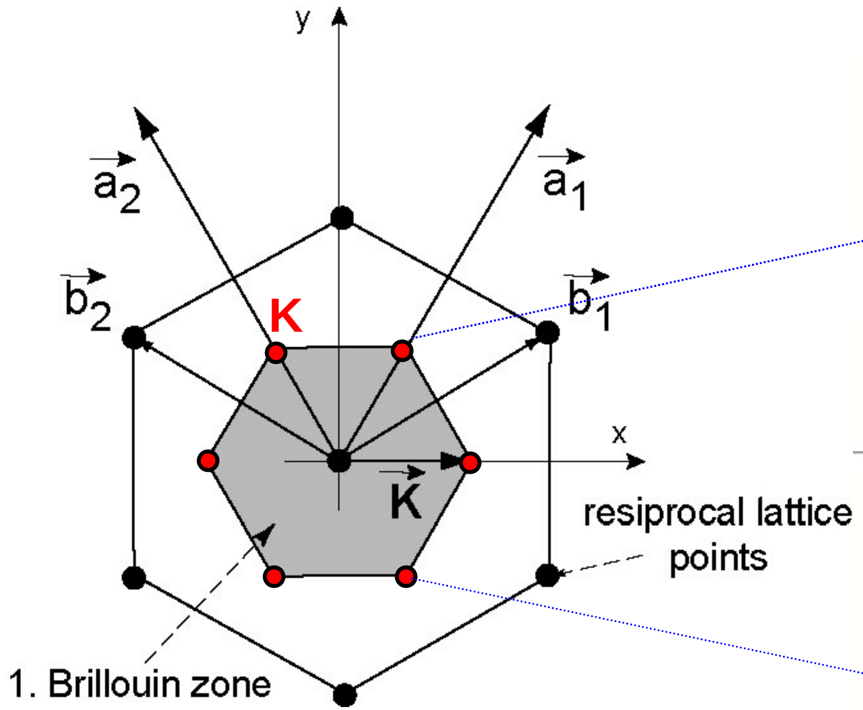

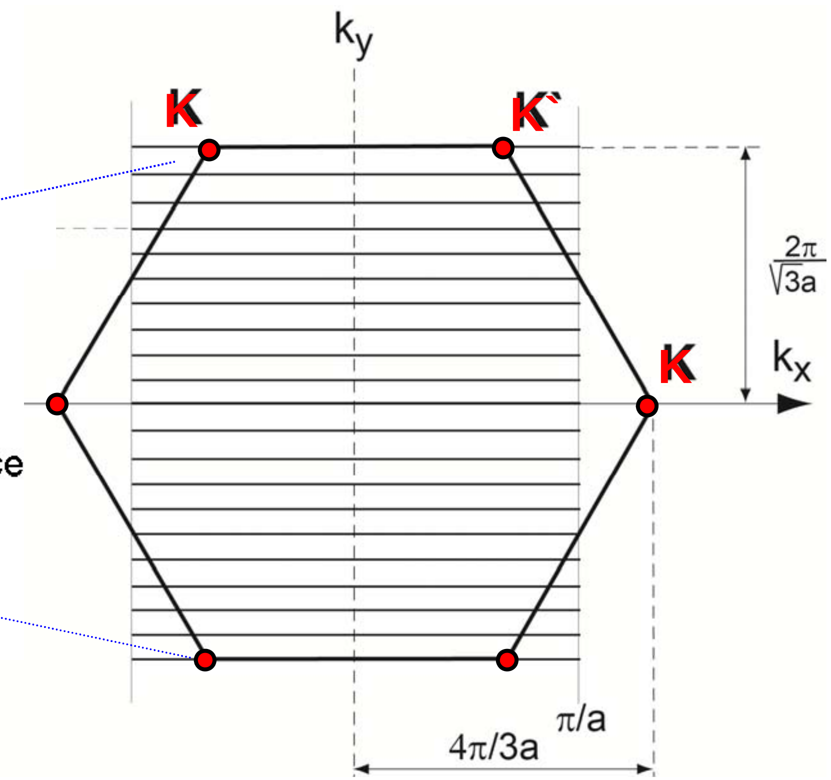

example: armchair CNT

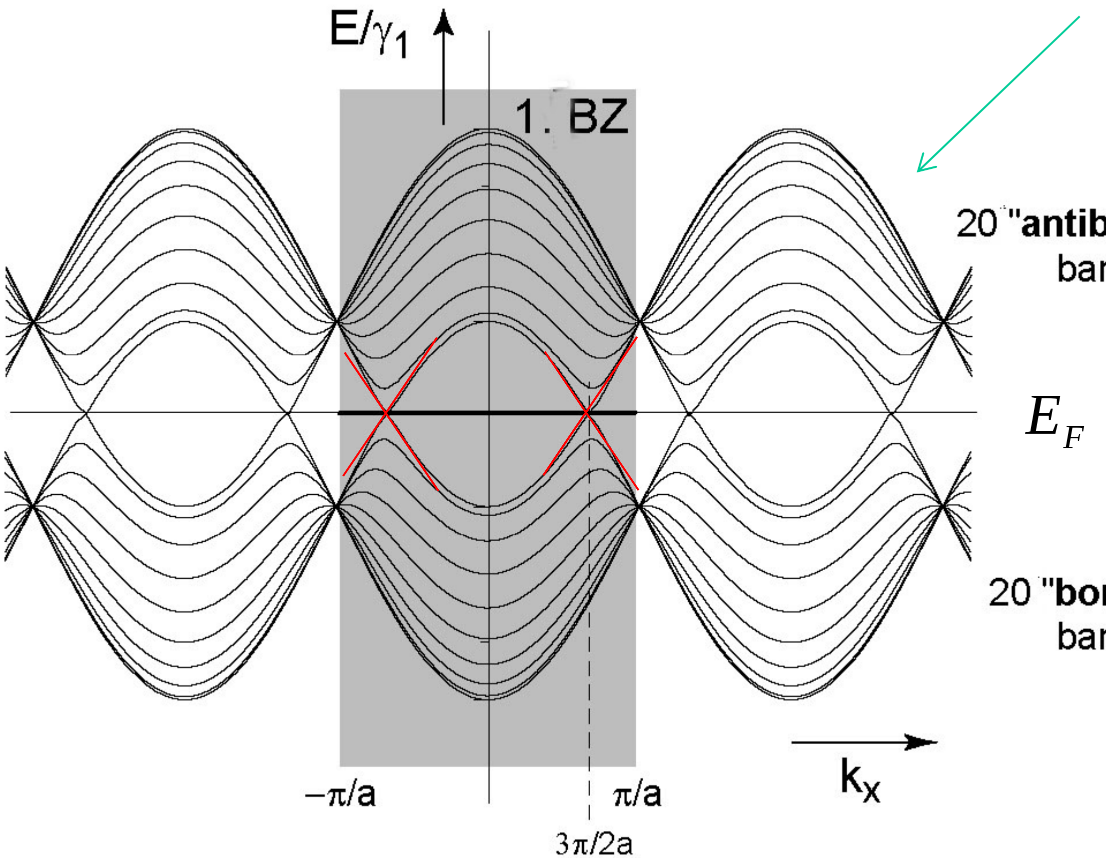

one can see 10 bands above E_F and 10 below E_F, each is two-fold degenerate (in addition to spin). There is a further one that crosses E_F. This one is **not** two-fold degenerate.

undoped Fermi energy, also known as the **charge neutrality point** (CNP)

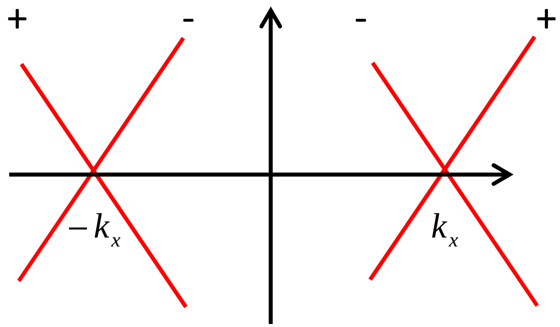

for low energies one can use the 1st order expansion. There are then **2 bands** (not counting spin) emerging from the K and K` valleys. There are two “rightmovers” and two “leftmovers”.

$$G = \frac{4e^2}{h}$$

how ballistic can it be?

VOLUME 87, NUMBER 10 PHYSICAL REVIEW LETTERS 3 SEPTEMBER 2001

Quantum Interference and Ballistic Transmission in Nanotube Electron Waveguides

Jing Kong, Erhan Yenilmez, Thomas W. Tombler, Woong Kim, and Hongjie Dai
Department of Chemistry and Laboratory for Advanced Materials, Stanford University, Stanford, California 94305

Robert B. Laughlin
Department of Physics, Stanford University, Stanford, California 94305

Lei Liu, C. S. Jayanthi, and S. Y. Wu
Department of Physics, University of Louisville, Louisville, Kentucky 40292
(Received 27 February 2001; published 16 August 2001)

The electron transport properties of well-contacted individual single-walled carbon nanotubes are investigated in the ballistic regime. Phase coherent transport and electron interference manifest as conductance fluctuations as a function of Fermi energy. Resonance with standing waves in finite-length tubes and localized states due to imperfections are observed for various Fermi energies. Two units of quantum conductance $2G_0 = 4e^2/h$ are measured for the first time, corresponding to the maximum conductance limit for ballistic transport in two channels of a nanotube.

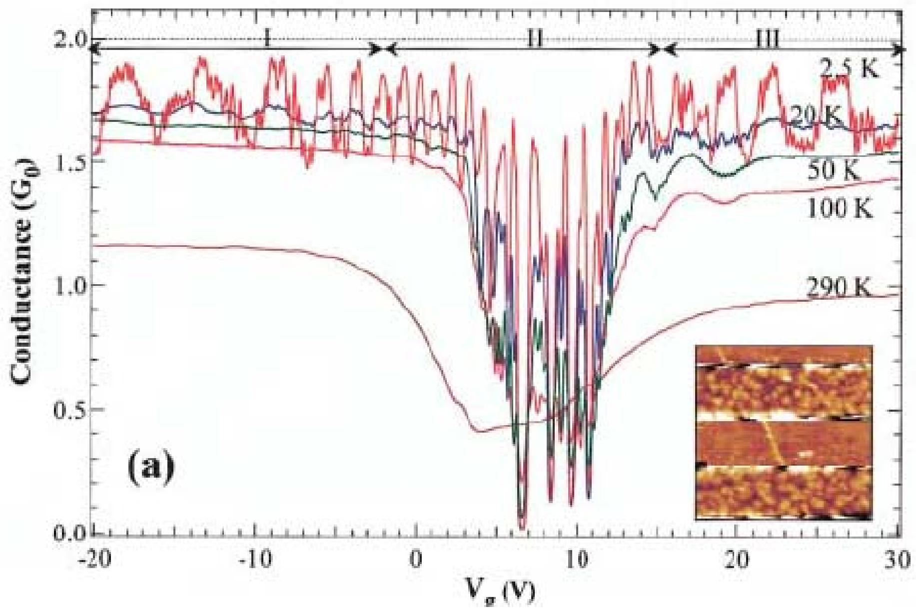

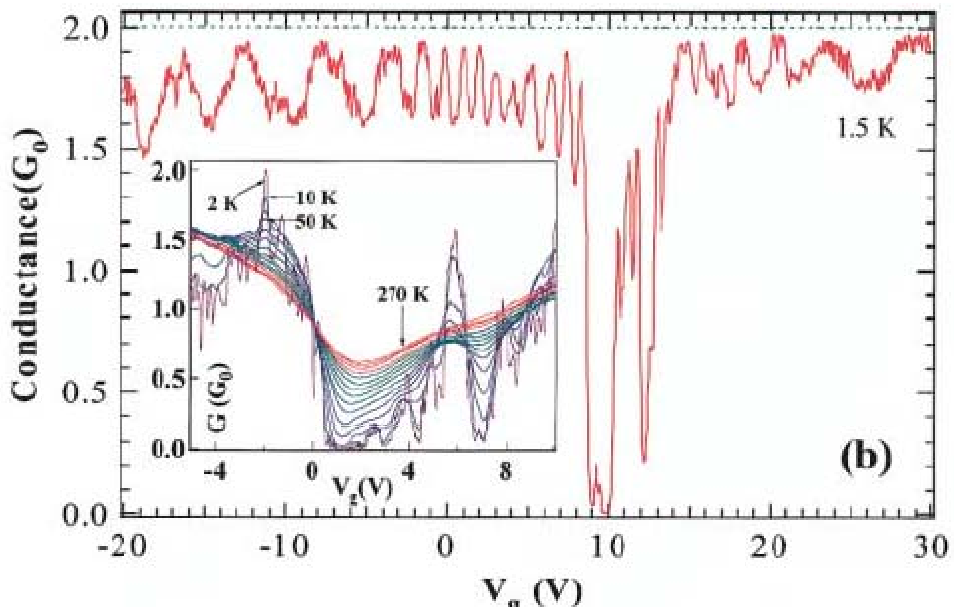

Data CNT from our own lab

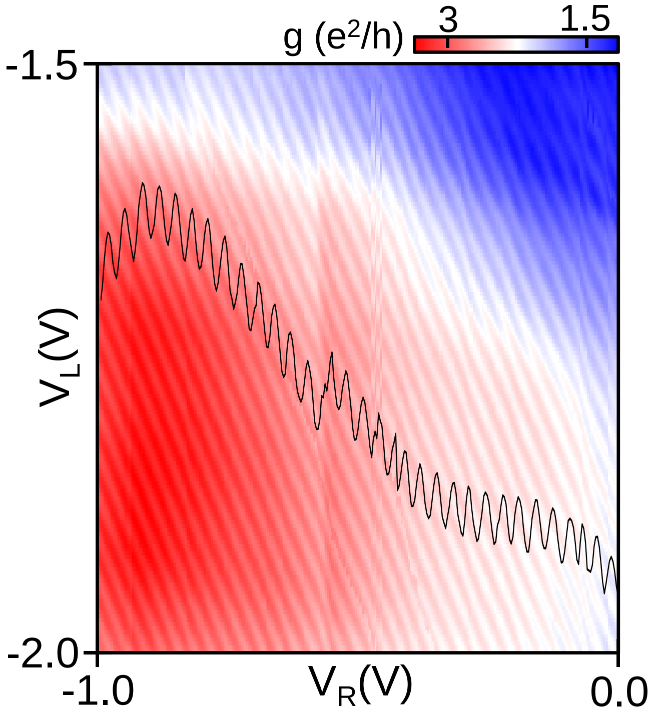

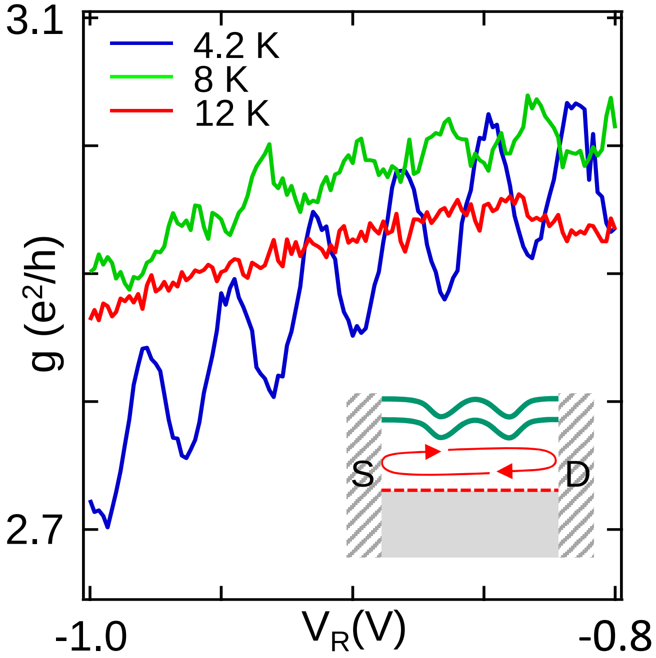

Transmission probability T > 0.8

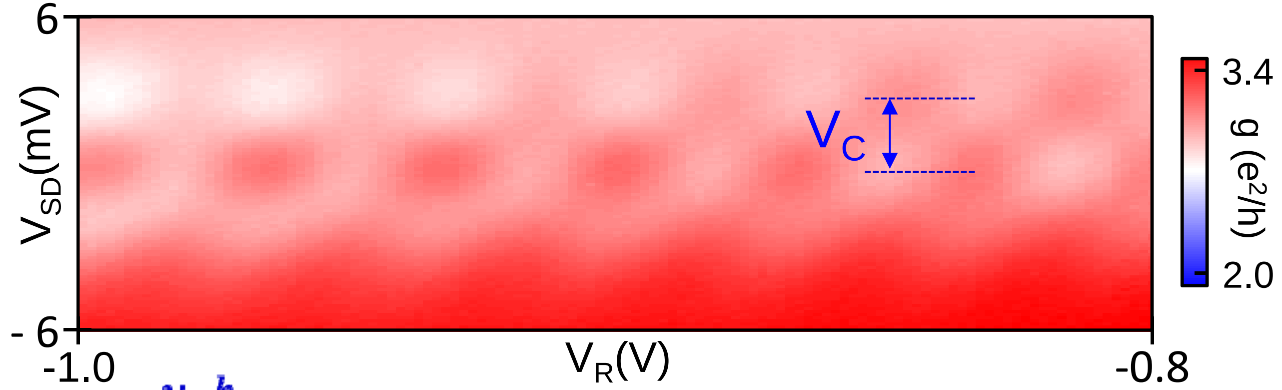

$L = \frac{\nu_F h}{2V_C}$ V_C ~ 3 mV, resulting in L ~ 700 nm

Minkyung Jung et al.

general CNT (chiral)

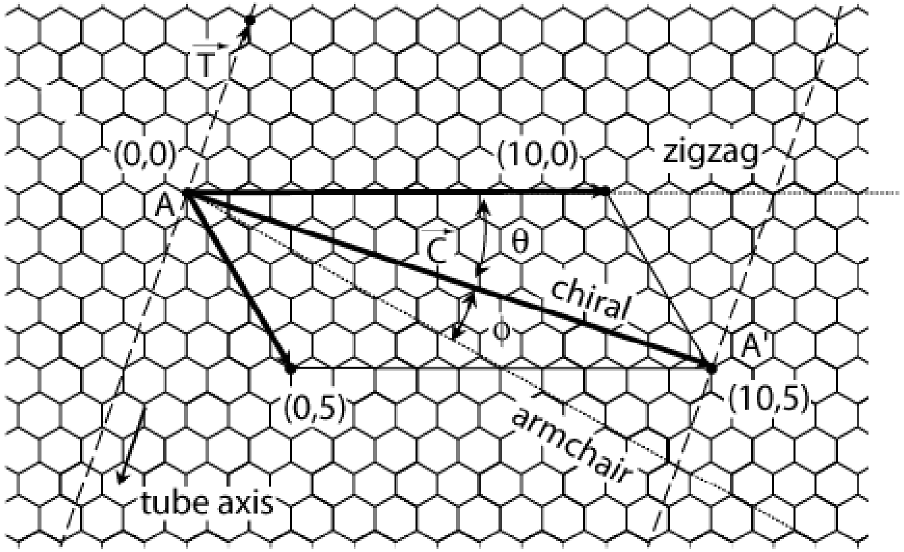

Graphene:

hexagonal lattice of carbon atoms

Chiral carbon nanotube

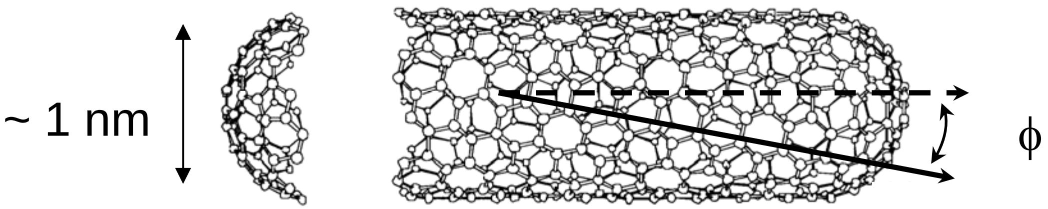

Atomically resolved STM image of a single-wall carbon nanotube.

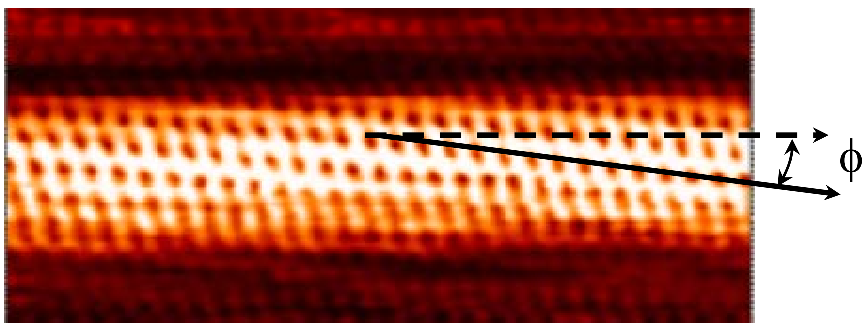

*Wildöer et al, Nature **391**, 59 (1998)*

general CNT (chiral)

- Armchair = All metallic
- The rest are metallic only when (m – n) = multiple of 3

blue ones are metallic
yellow ones are semiconductors

Zig-zag; (n,0) ; chiral angle = 0

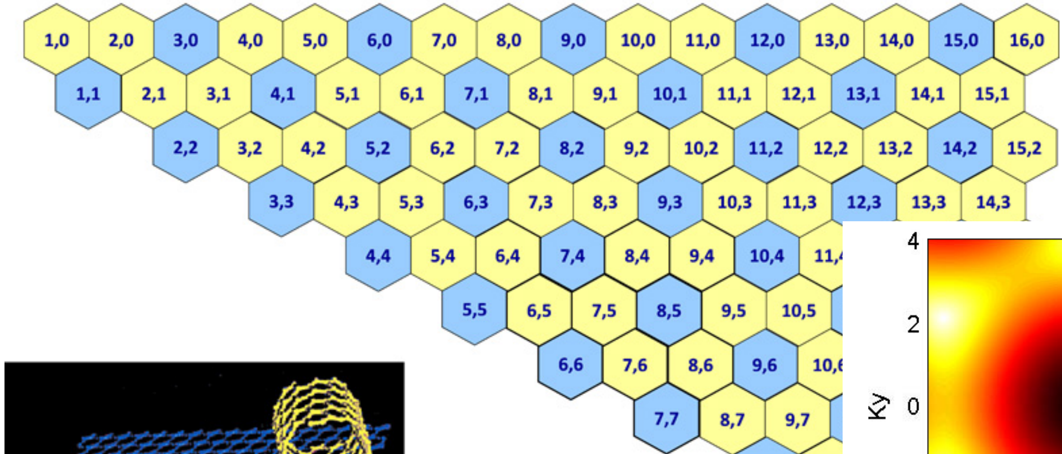

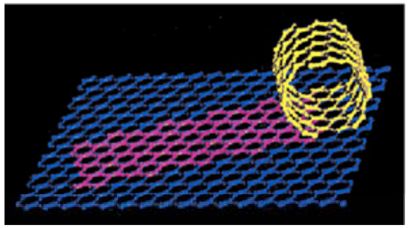

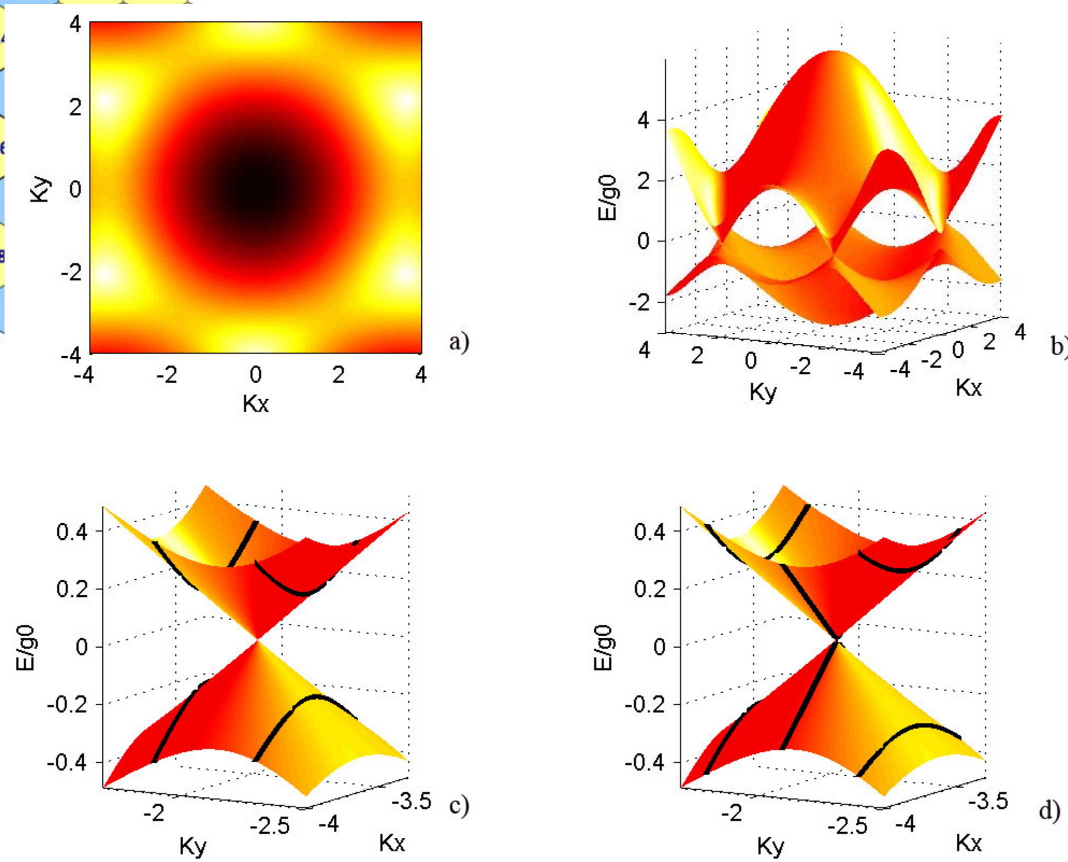

simplified band structure

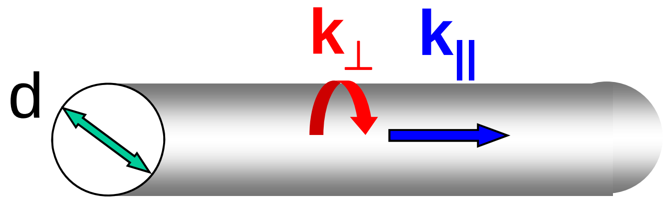

$$E_{2d}(\vec{k}) = \pm\hbar v_F \left|\vec{k}\right|$$

($v_F \cong 10^6$ m/s)

$k_\perp \pi d = 2\pi m$, m=0,1,2...

metallic

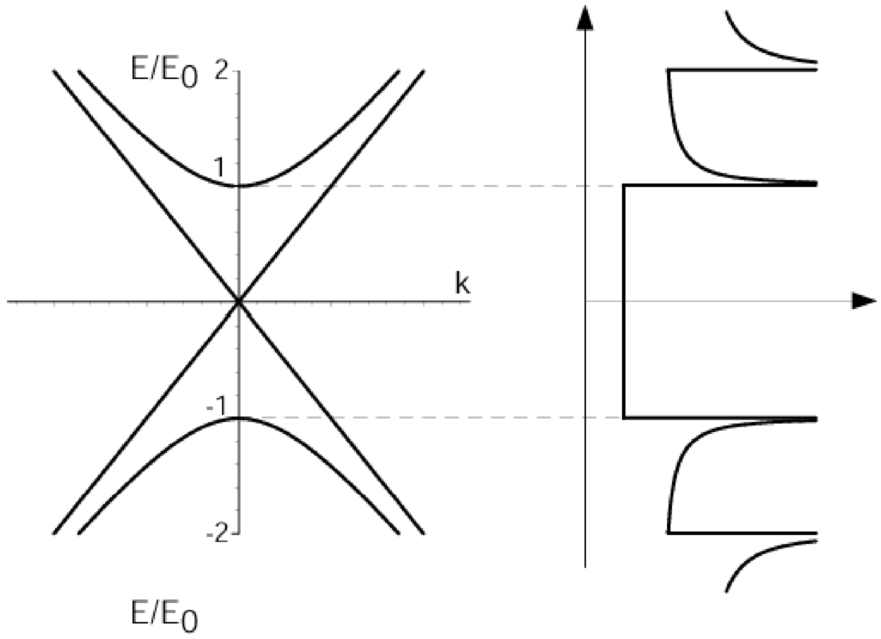

semiconducting

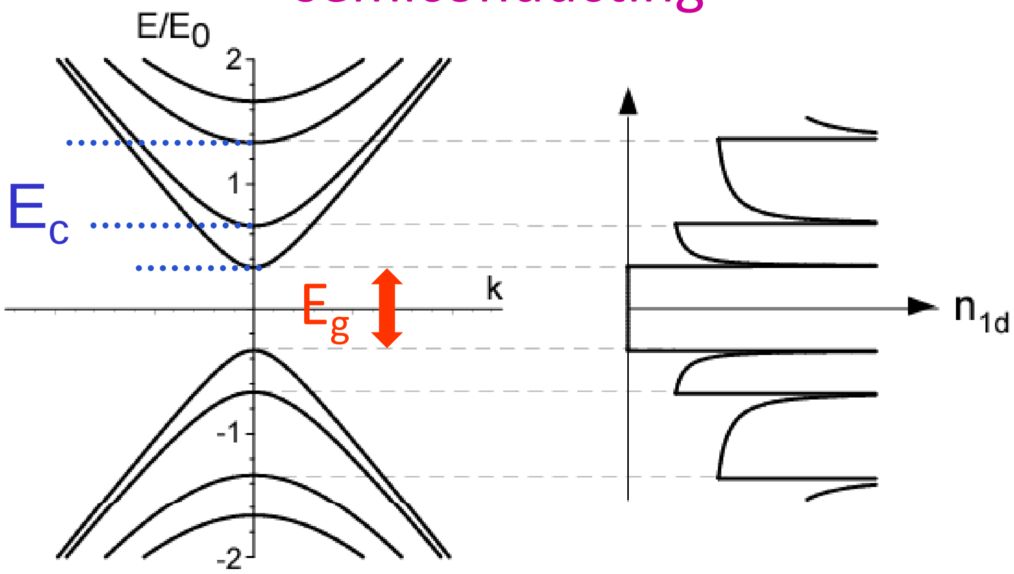

$E_0 \cong 1.3$ eV (1 nm diameter)

$E_0 \propto 1/d$

$E_g = 2E_0/3$

E_c = cut-off energies of 1d „subbands“

ideally G = 0 or G = $4e^2/h$

Graphene nanoribbons

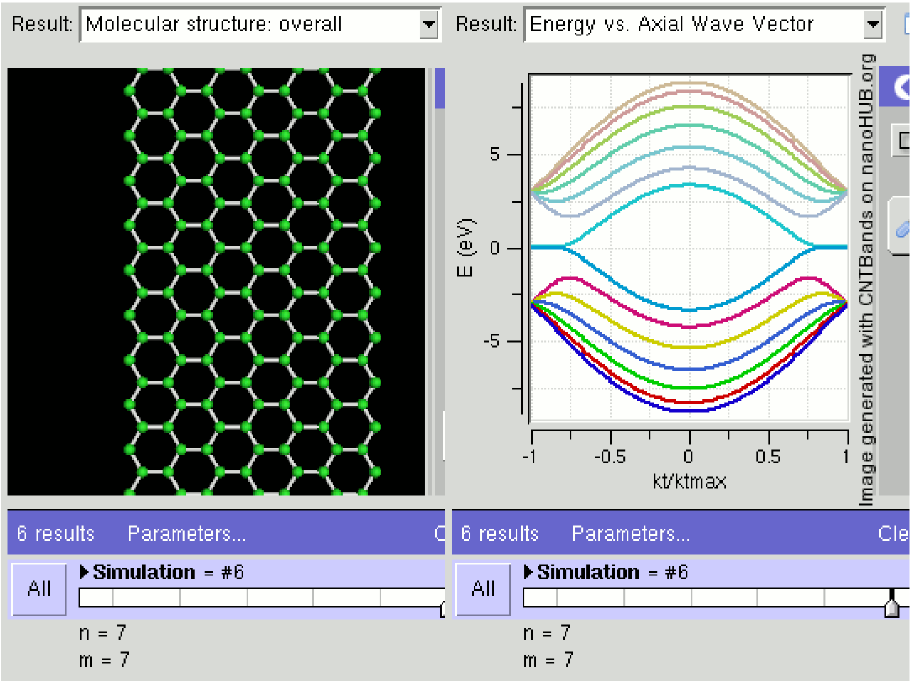

GNR band structure for zig-zag type (in CNT notation, this is armchair). Tight binding calculations predict that zigzag type is always metallic

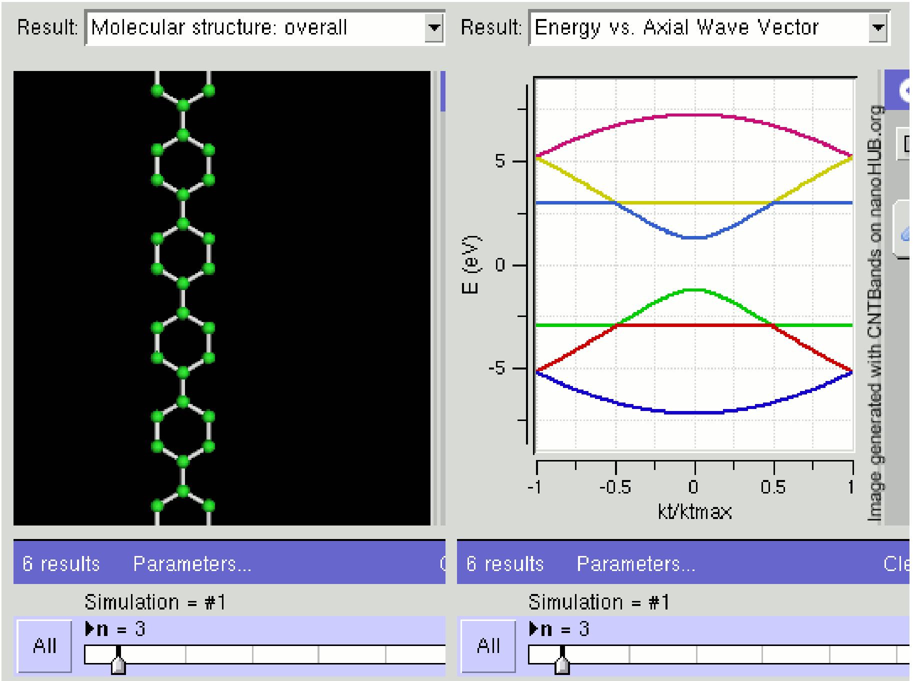

GNR band structure for armchair type. Tight binding calculations show that armchair type can be semiconducting or metallic depending on width.

http://en.wikipedia.org/wiki/Graphene_nanoribbons

4. Bandstructure of bilayer (multilayer) graphene

Bandstructure of bilayer graphene

bilayer graphene = 2 sheets of graphene acting like a single 2D system

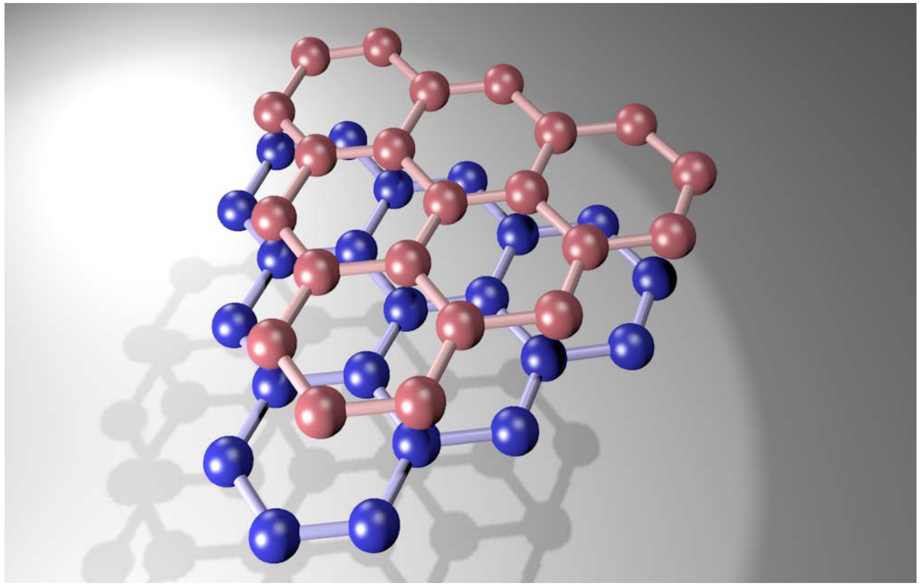

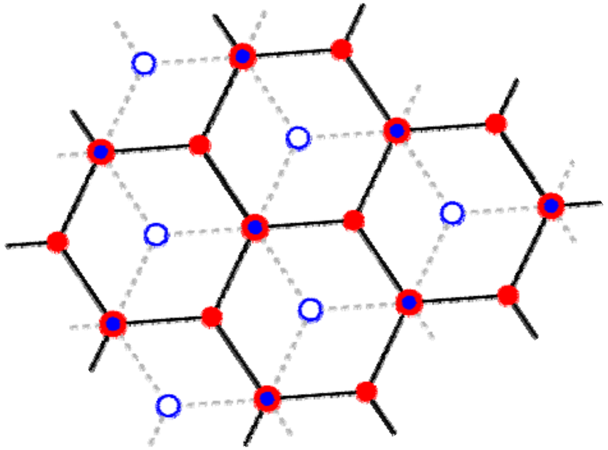

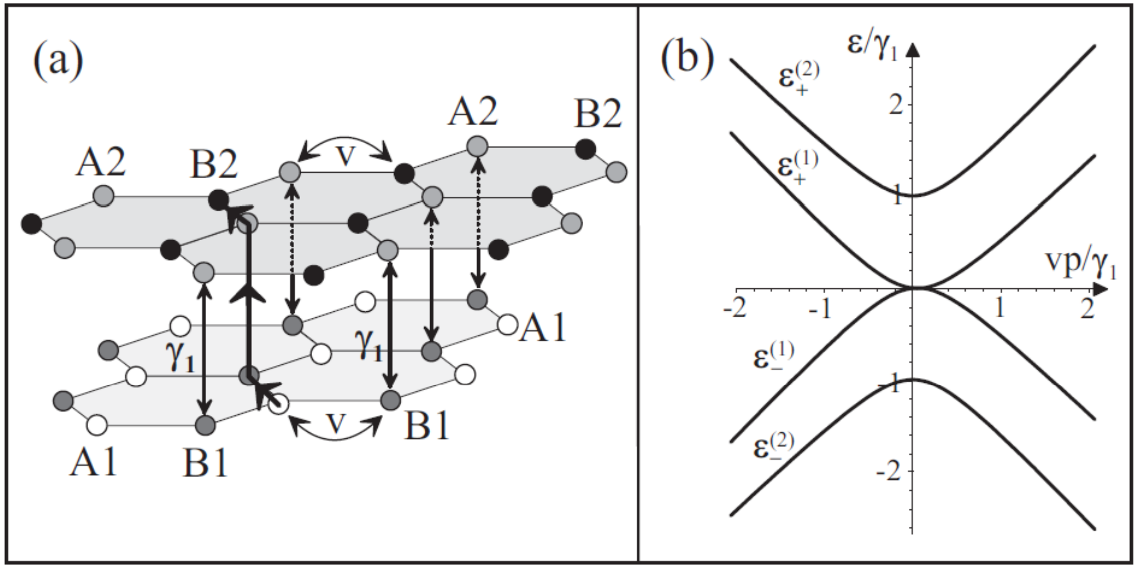

$$H = \begin{pmatrix} 0 & v\pi^+ & 0 & 0 \\ v\pi & 0 & \gamma_1 & 0 \\ 0 & \gamma_1 & 0 & v\pi^+ \\ 0 & 0 & v\pi & 0 \end{pmatrix}$$

in the basis A_1, $\tilde{B}_1$, $\tilde{A}_2$, B_2

left: band structure for u=0 (no interlayer electric field). Bands have massive, but still they are chiral)

Bandstructure of bilayer graphene

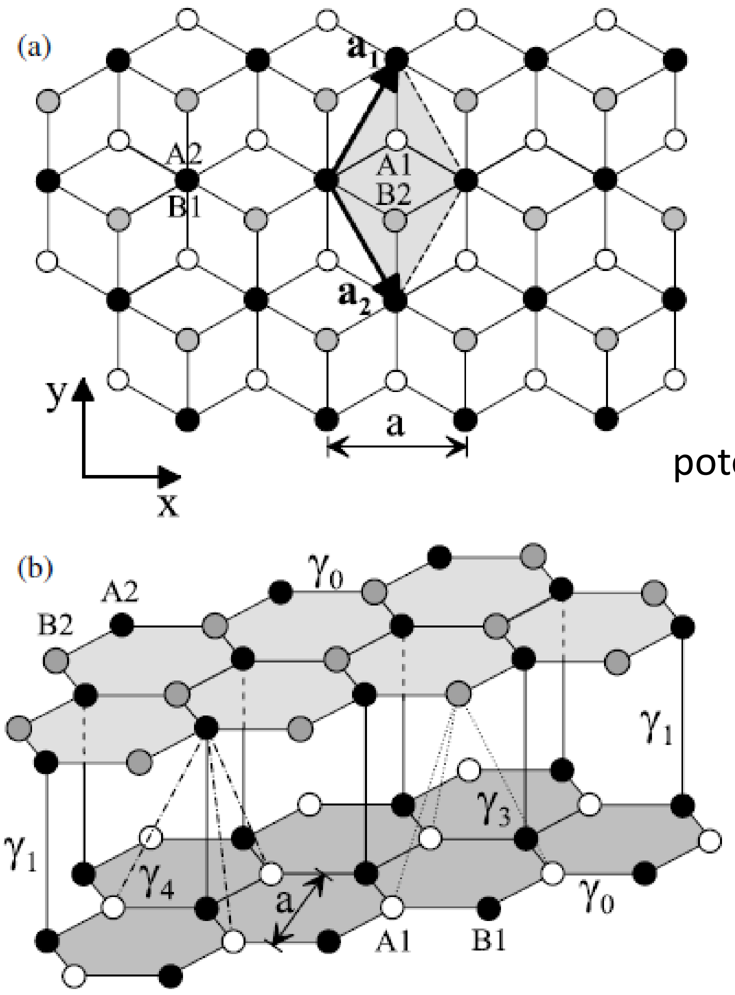

Figure 2. (*a*) Plan and (*b*) side view of the crystal structure of bilayer graphene. Atoms *A*1 and *B*1 on the lower layer are shown as white and black circles, *A*2, *B*2 on the upper layer are black and grey, respectively. The shaded rhombus in (*a*) indicates the conventional unit cell.

$$H = \begin{bmatrix} \frac{u}{2} & v\pi^\dagger & 0 & \\ v\pi & \frac{u}{2} & \gamma_1 & 0 \\ 0 & \gamma_1 & -\frac{u}{2} & v\pi^\dagger \\ & 0 & v\pi & -\frac{u}{2} \end{bmatrix}, \quad \begin{cases} \pi = p_x + ip_y \\ v = \frac{\sqrt{3}}{2}\frac{a\gamma_0}{\hbar} \sim 10^6 \text{ m/s} \end{cases}$$

potential difference *u* between layers

opens bandgap

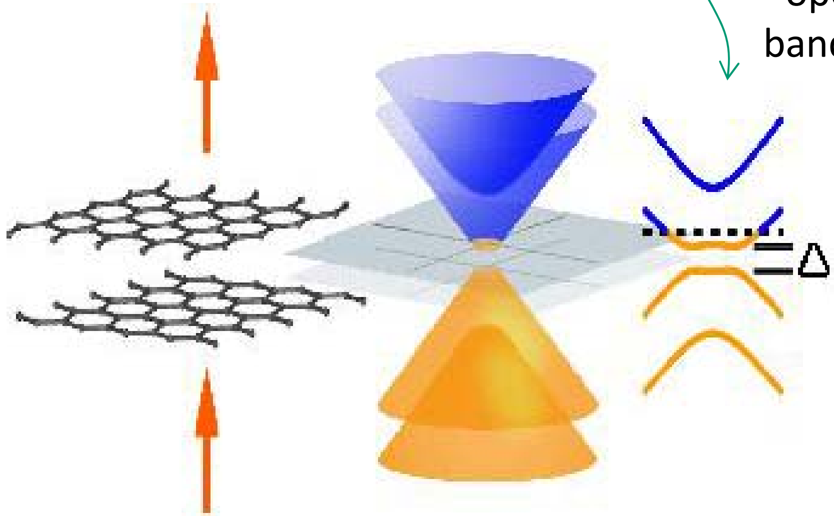

Bandstructure of bilayer graphene

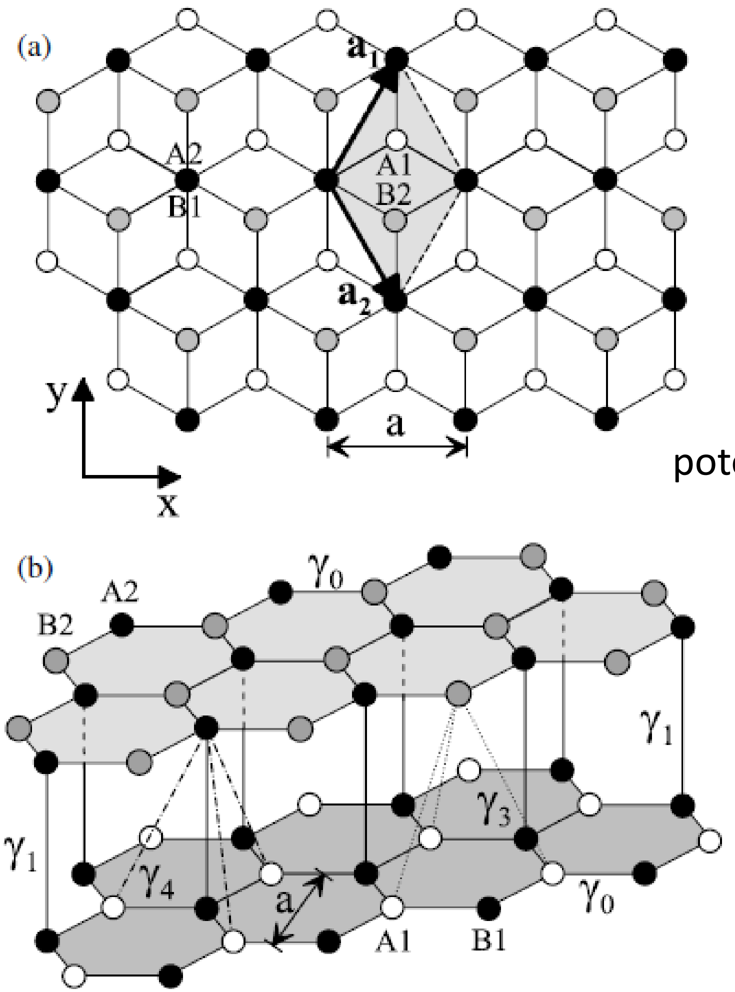

Figure 2. (*a*) Plan and (*b*) side view of the crystal structure of bilayer graphene. Atoms $A1$ and $B1$ on the lower layer are shown as white and black circles, $A2$, $B2$ on the upper layer are black and grey, respectively. The shaded rhombus in (*a*) indicates the conventional unit cell.

“skew” coupling

$$H = \begin{bmatrix} \frac{u}{2} & v\pi^\dagger & 0 & v_3\pi \\ v\pi & \frac{u}{2} & \gamma_1 & 0 \\ 0 & \gamma_1 & -\frac{u}{2} & v\pi^\dagger \\ v_3\pi^\dagger & 0 & v\pi & -\frac{u}{2} \end{bmatrix}, \quad \begin{cases} \pi = p_x + ip_y \\ v = \frac{\sqrt{3}}{2}\frac{a\gamma_0}{\hbar} \sim 10^6 \text{ m/s} \\ v_3 = \frac{\sqrt{3}}{2}\frac{a\gamma_3}{\hbar} \sim 0.1\ v \end{cases}$$

potential difference *u* between layers

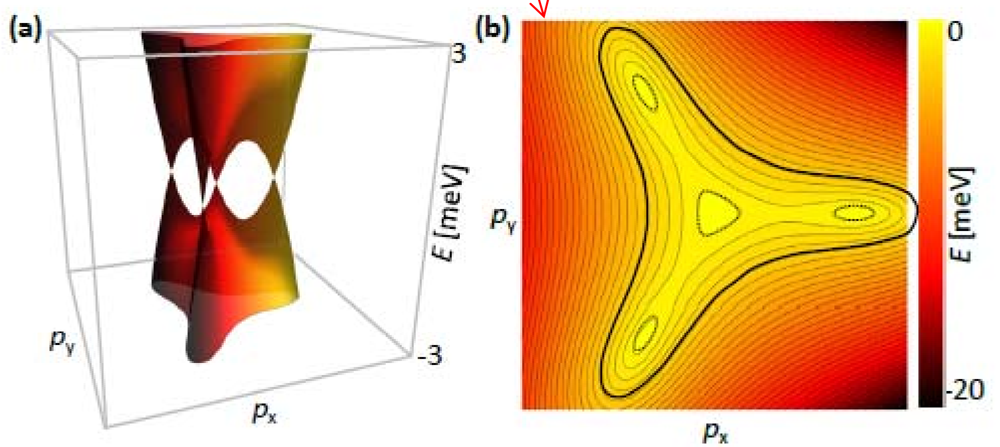

v_3 term can close the gap again. Effect known as trigonal warping and results into a so called **Lifshitz transition**

McCann Rep. Prog. Phys. 76, 056503 (2013)

5. Charaterization

Bandstructure of bilayer graphene

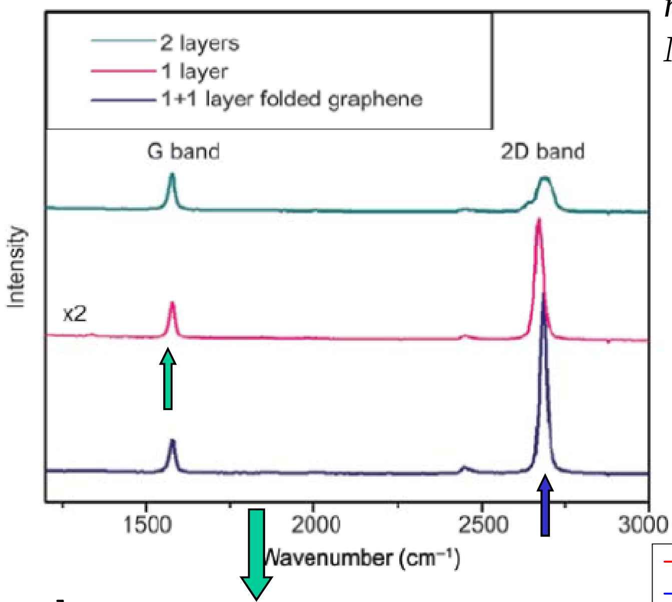

ref.: Zhenhua et al.
Nano Re. V1, p273 (2008)

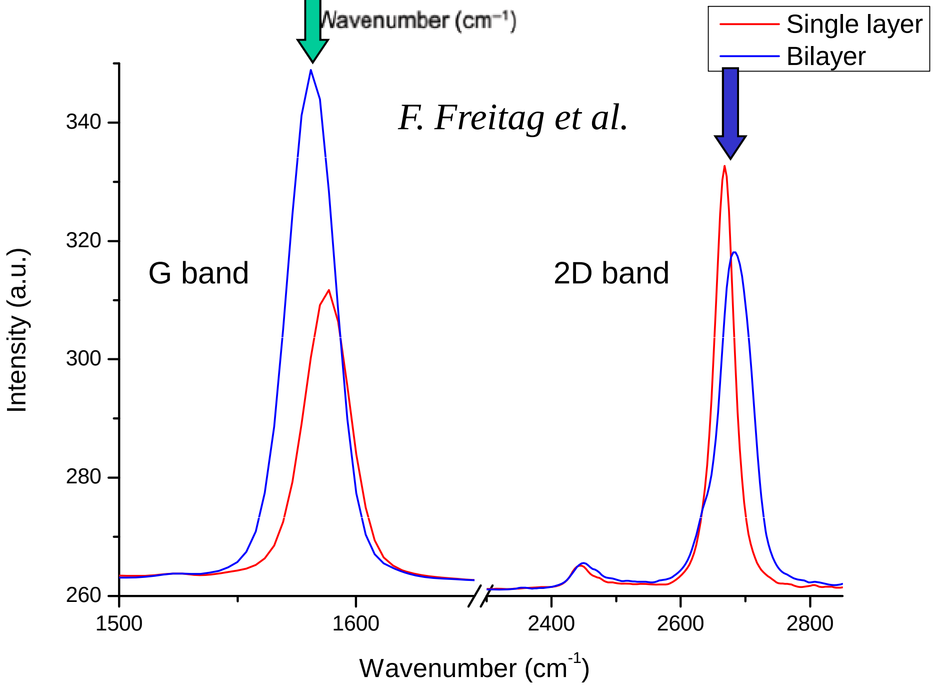

F. Freitag et al.

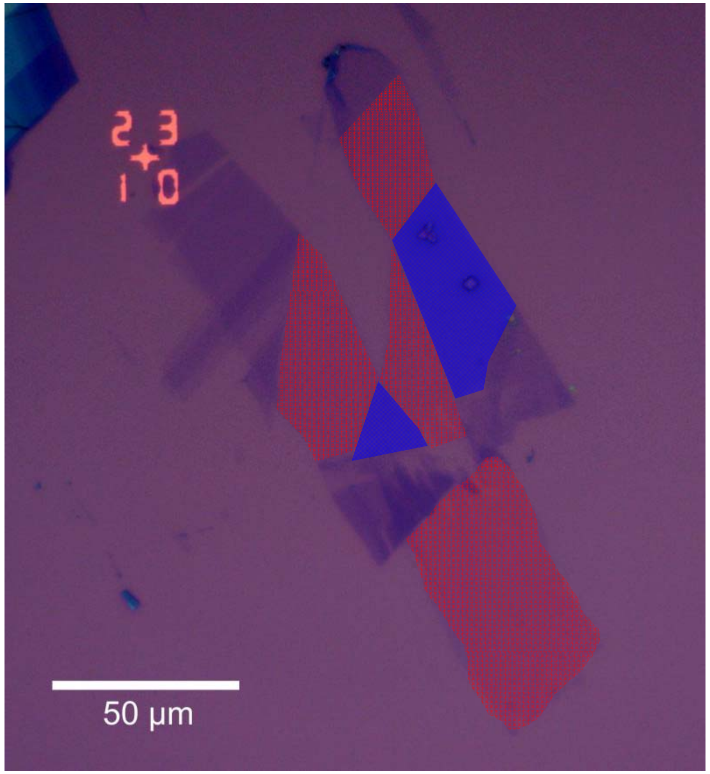

locate flakes in optical microscope...

... and identify the number of layer with Raman spectroscopy.
(also reveals chemical doping and contaminations)

Quantum Hall effect in monolayer graphene

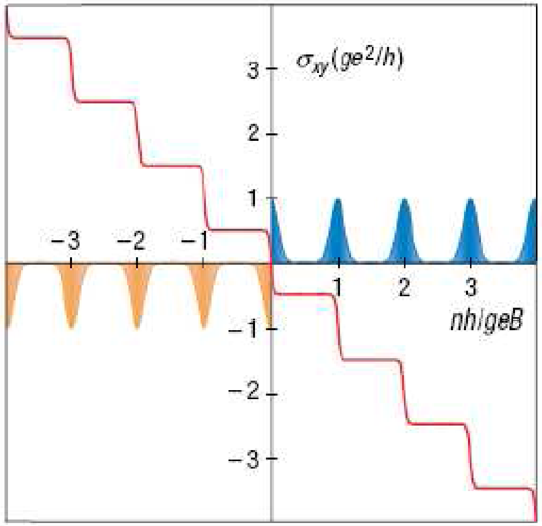

Landau levels

$$\omega_c = \pm v_F \sqrt{2e\hbar B|n|}$$

$$\sigma_{xy} = g(n+1/2)\frac{e^2}{h}$$

$$\sigma_{xy} = \nu \frac{e^2}{h} \qquad \nu=2,6,10\ldots$$

$$\Delta\sigma_{xy} = \frac{4e^2}{h}$$

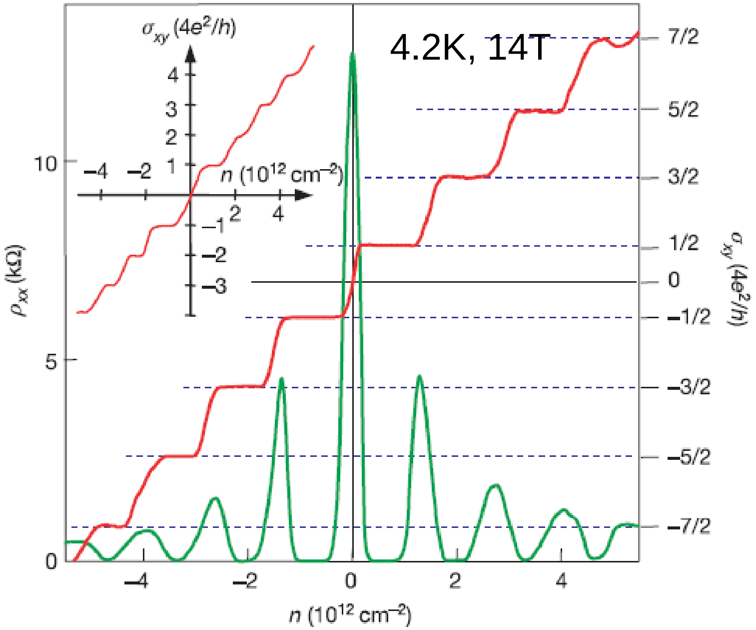

K. Novoselov et al. Nature 438, 197-200 (2005)

Quantum Hall effect in **bilayer** graphene

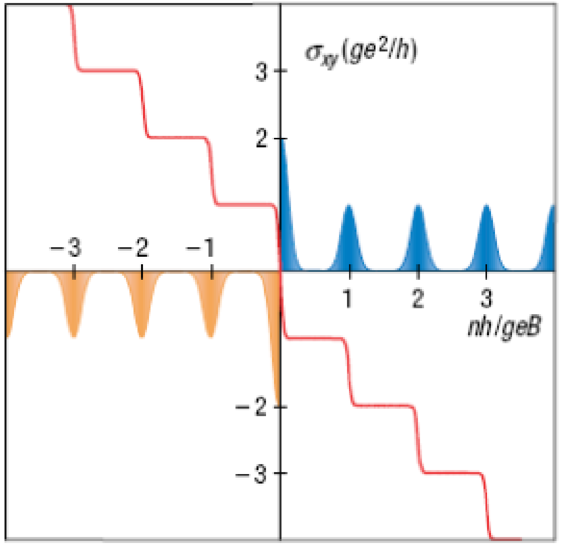

Landau levels

still at zero-energy LL

$$\sigma_{xy} = \nu \frac{e^2}{h} \qquad \nu=4,8,12$$

$$\Delta\sigma_{xy} = \frac{4e^2}{h}$$

zero-energy LL has 8-fold degeneracy

→ expect also broken symmetry states in clean samples

Feldman et al. Nature Phys. 5, p889 (2009)
Zhao et al. Phys. Rev.Lett. 104, p066801 (2010)

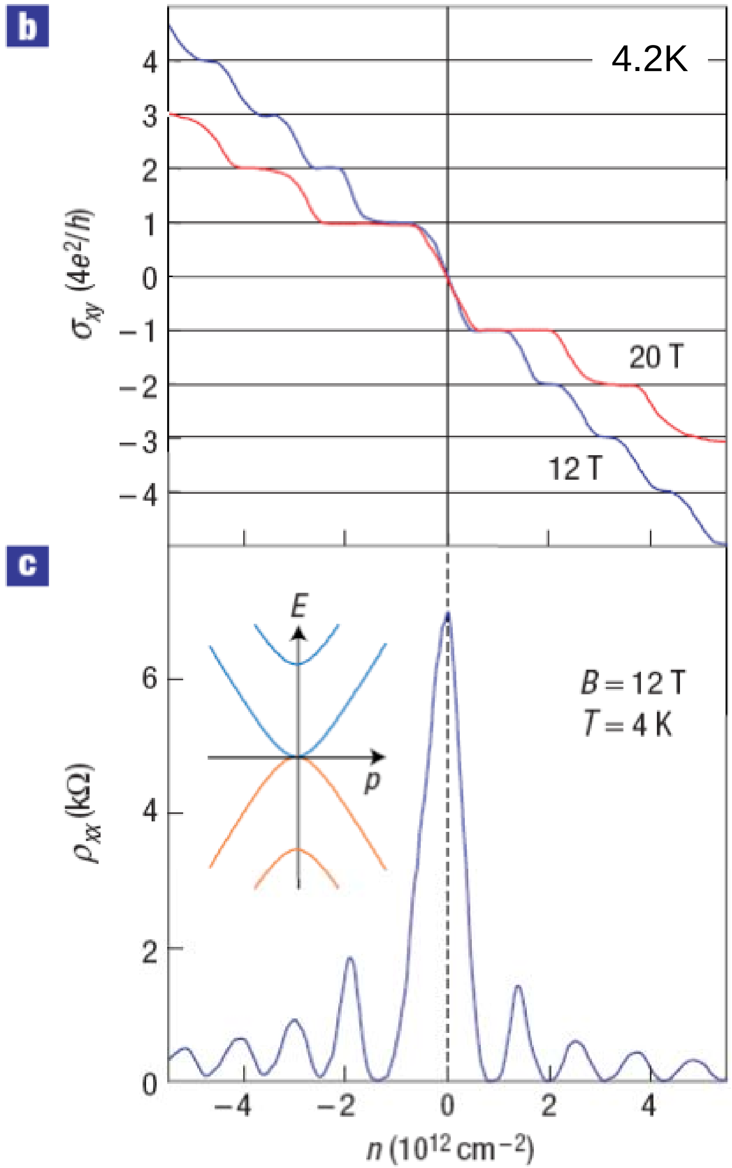

K. Novoselov et al. Nat. Phys. 2, 177 (2006)

from our lab (very recent)

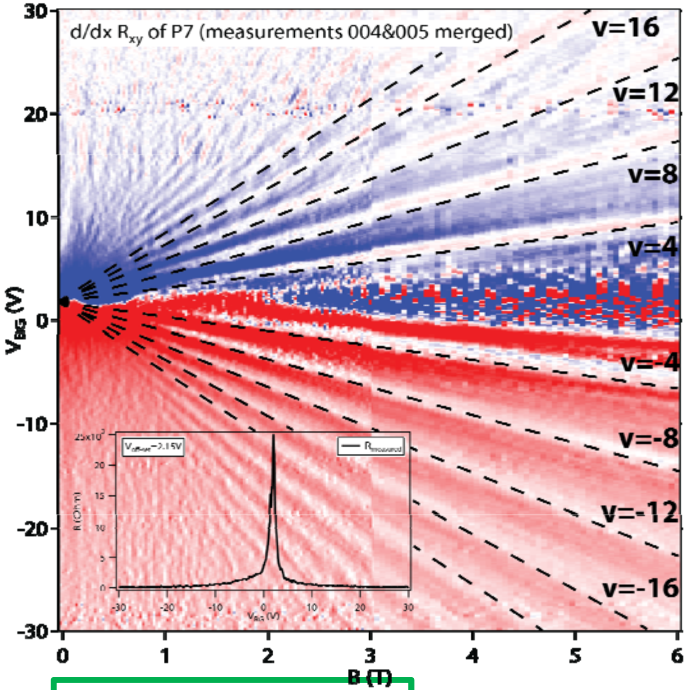

Filling-factors:
ν=±4, ±8, ±12,...

-> **BLG** (bilayer)

L. Wang, et al., *Science,* **342,** 614 (2013);

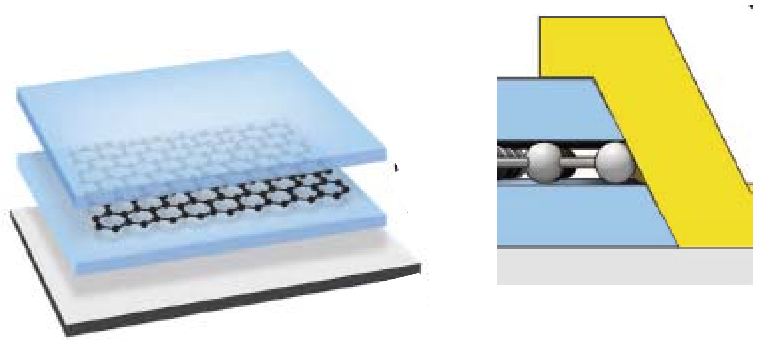

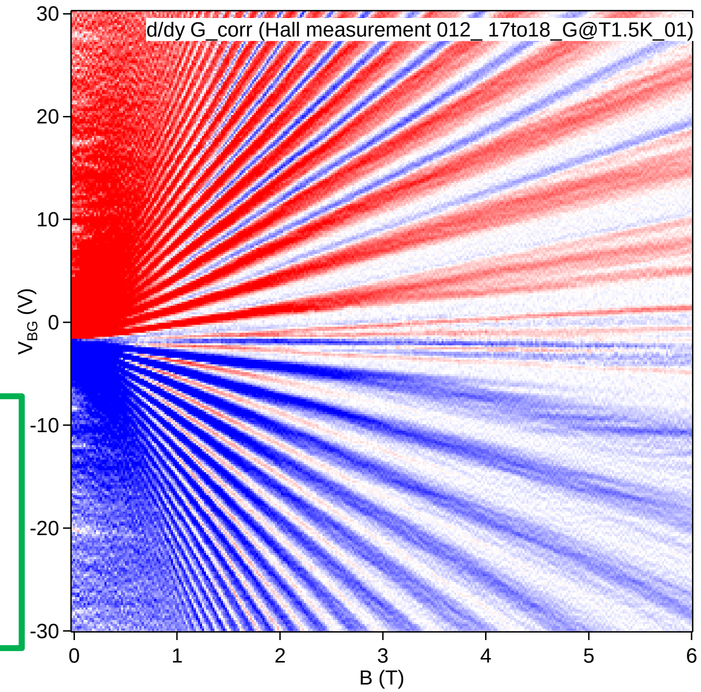

Filling-factors:
ν=±2, ±6, ±10,...

-> **SLG** (single layer)

C. Handschin, B. Fülöp, P. Makk et al.

6. Electron optics in ballistic graphene

Electron optics in graphene

Unipolar interface (nn’ or pp’)

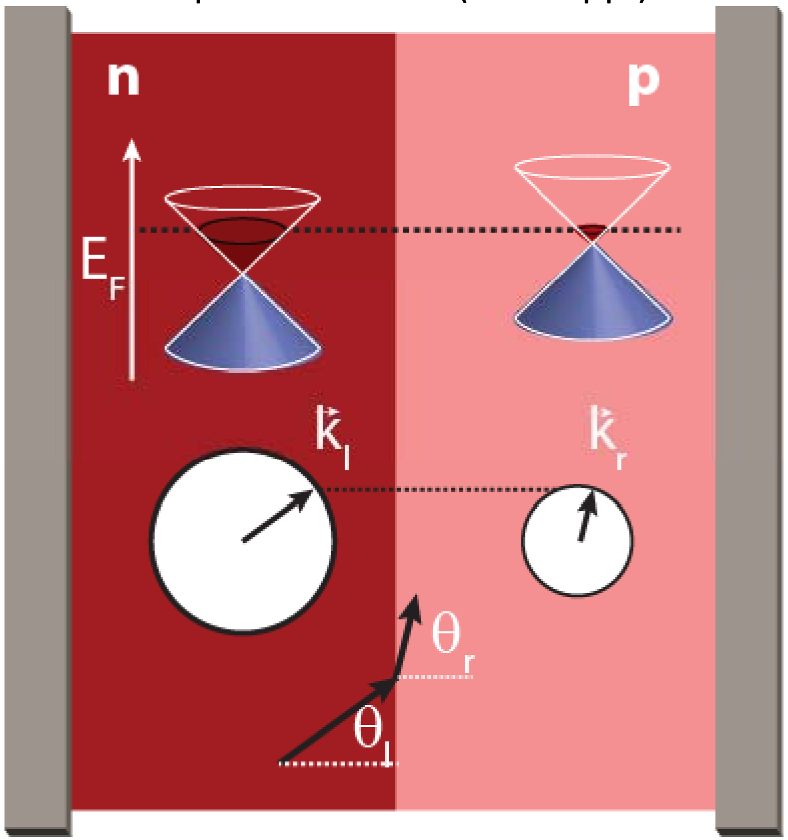

Conservation of transverse momentum

Snell’s law

$$\vec{k}_l \sin\theta_l = \vec{k}_r \sin\theta_r$$

Bipolar interface (nn’ or pp’)

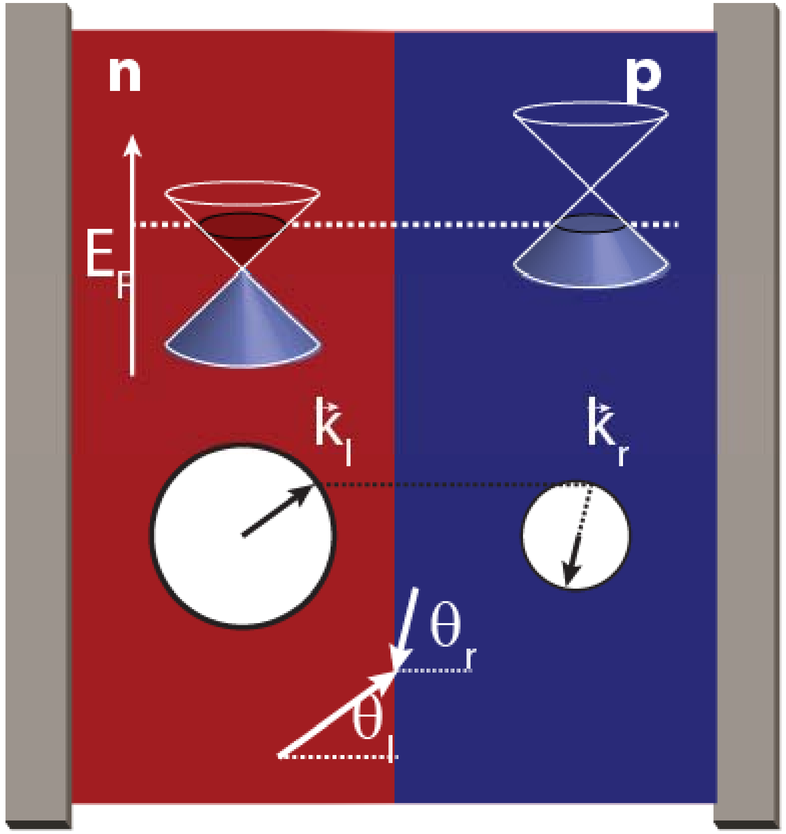

Conservation of transverse momentum

anomalous Snell’s law

$$\vec{k}_l \sin\theta_l = -\vec{k}_r \sin\theta_r$$

Electron optics in graphene

reason: velocity is opposite to wavevector in p-doped regions

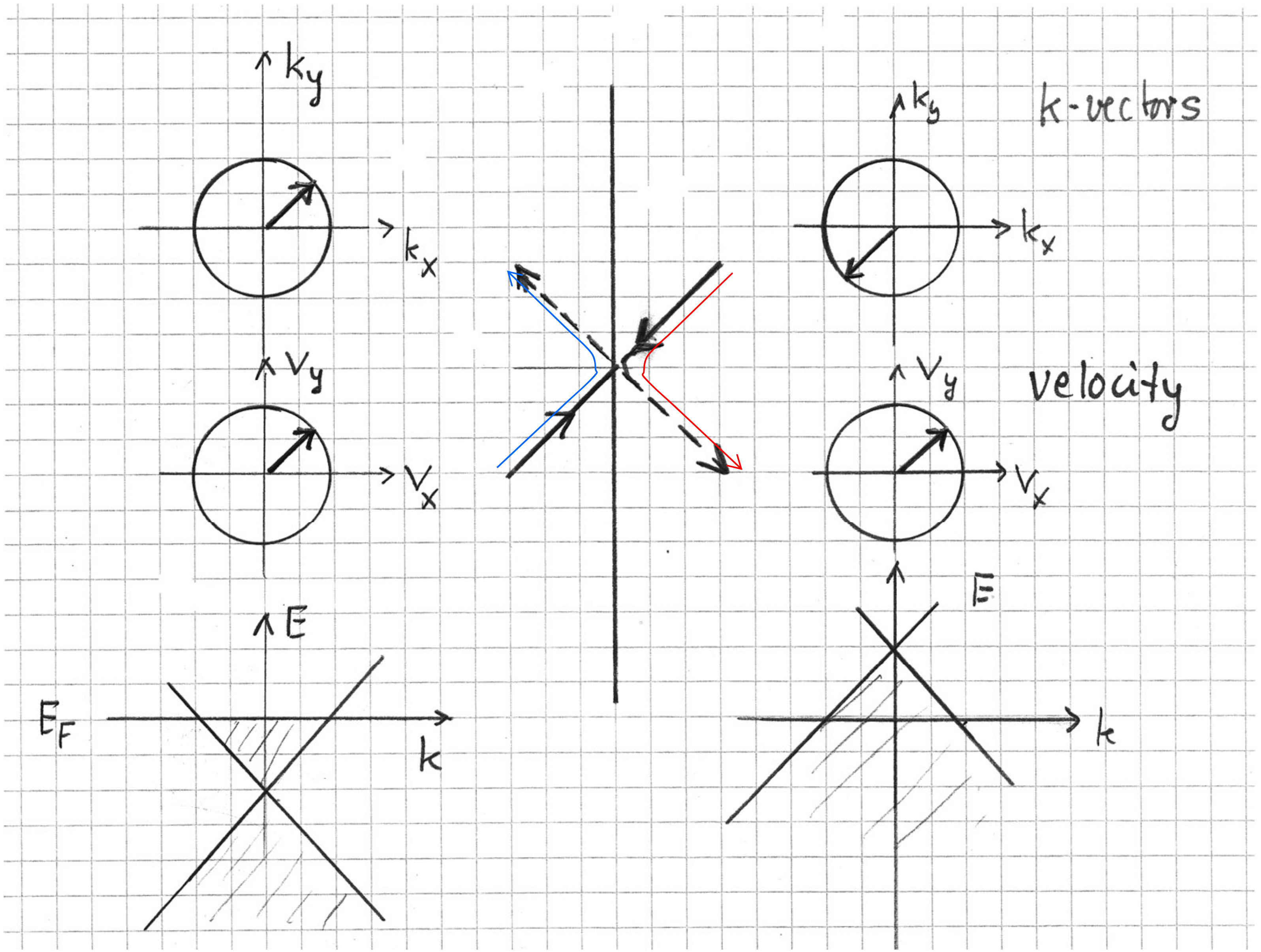

Electron optics in graphene

wavefunctions at the two sides of a sharp potential step:

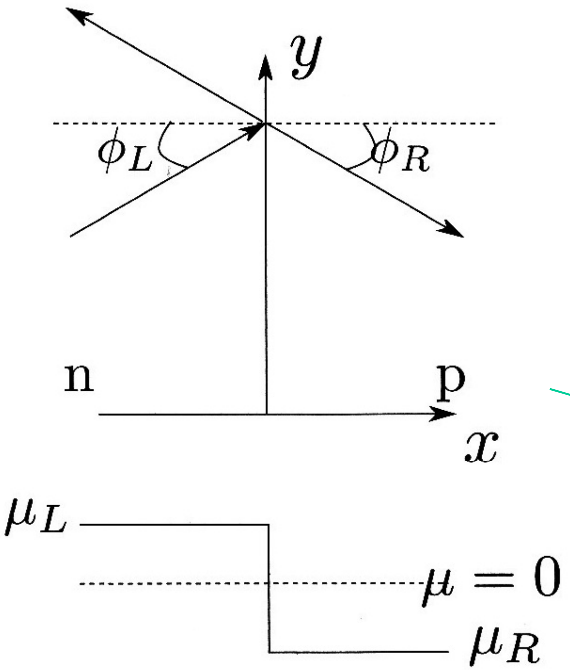

Fig. 10.13 Graphene np junction.

taken from Heikkilä book

matching wavefunction:

$$|t|^2 = \frac{\cos^2(\phi_L)}{\cos^2(\phi_L/2 - \phi_R/2)}.$$

in particular, when μL=-μR, the two angles are the same, yielding $|t|^2 = \cos^2(\phi_L)$

$$\psi_L(x,y) = \frac{1}{\sqrt{2}}\begin{pmatrix} 1 \\ -e^{i\phi_L} \end{pmatrix} e^{i(k_x^L x + k_y y)} + \frac{r}{\sqrt{2}}\begin{pmatrix} 1 \\ -e^{i(\pi-\phi_L)} \end{pmatrix} e^{i(-k_x^L x + k_y y)}$$

$$\psi_R(x,y) = \frac{t}{\sqrt{2}}\begin{pmatrix} 1 \\ e^{i(\pi-\phi_R)} \end{pmatrix} e^{i(-k_x^R x + k_y y)}. \qquad (10.35)$$

solution chosen so that helicity is correct on the right side

electron diffraction

refraction at an unipolar interface

sharp unipolar interface

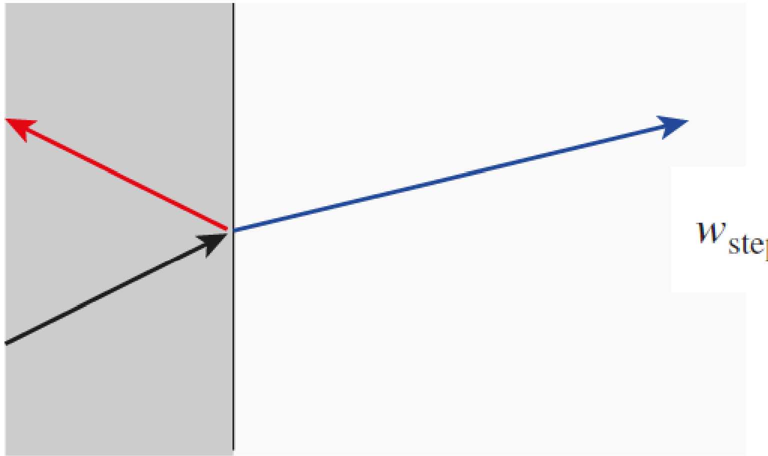

$$w_{\text{step}}(\theta) = \cos^2\theta$$

refraction at a bipolar interface

sharp bipolar interface

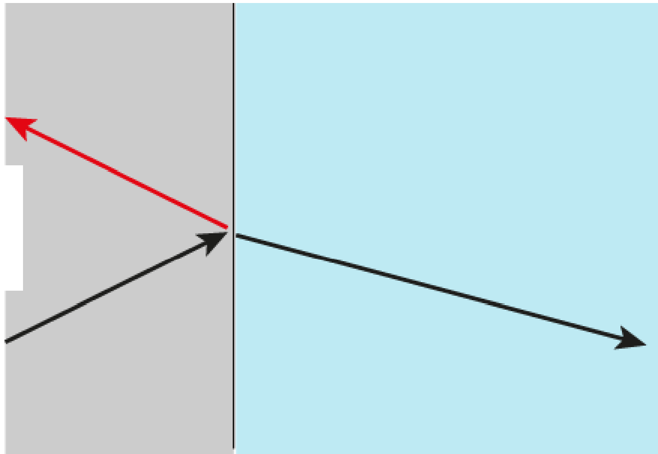

smooth unipolar interface

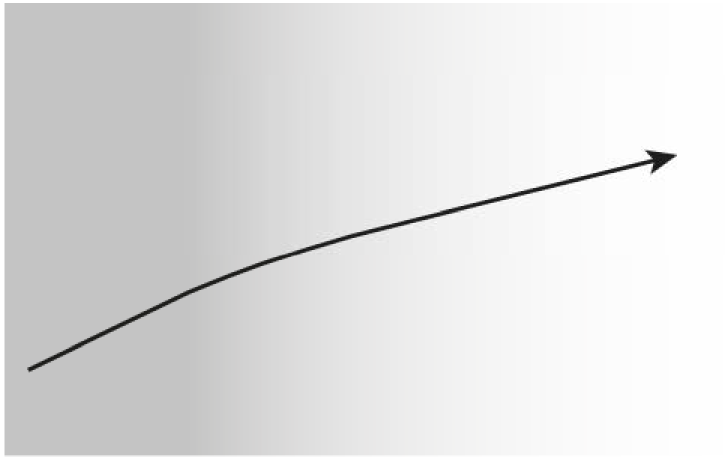

transmission probability ~1

smooth bipolar interface

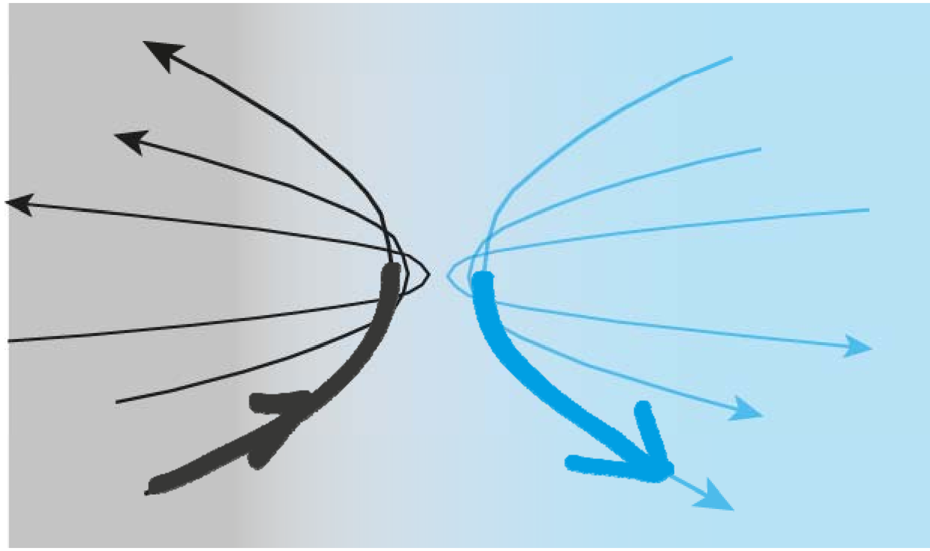

transmission probability ?

Electron optics in graphene

PHYSICAL REVIEW B **74**, 041403(R) (2006)

Selective transmission of Dirac electrons and ballistic magnetoresistance of *n-p* junctions in graphene

Vadim V. Cheianov and Vladimir I. Fal'ko
Department of Physics, Lancaster University, Lancaster, LA1 4YB, United Kingdom
(Received 23 March 2006; revised manuscript received 21 May 2006; published 17 July 2006)

We show that an electrostatically created *n-p* junction separating the electron and hole gas regions in a graphene monolayer transmits only those quasiparticles that approach it almost perpendicularly to the *n-p* interface. Such a selective transmission of carriers by a single *n-p* junction would manifest itself in nonlocal magnetoresistance effect in arrays of such junctions and determines the unusual Fano factor in the current noise universal for the *n-p* junctions in graphene.

angle-filtering at sharp p-n interface: $w_{\text{step}}(\theta) = \cos^2 \theta$

in contrast, at a soft interface classically all trajectories are reflected

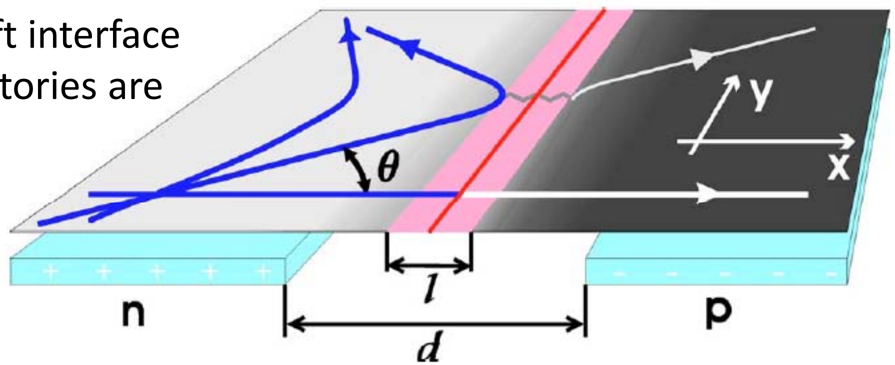

FIG. 1. (Color online) Angular dependence of quasiparticle transmission through the electrostatically generated *n-p* junction in graphene.

quantum-mechanically the particles **can tunnel** from one side to the other with probability:

$$w(\theta) = e^{-\pi(k_F d)\sin^2 \theta}.$$

Klein effect
Klein tunneling

Electron optics in graphene

in contrast, at a soft interface classically all trajectories are reflected

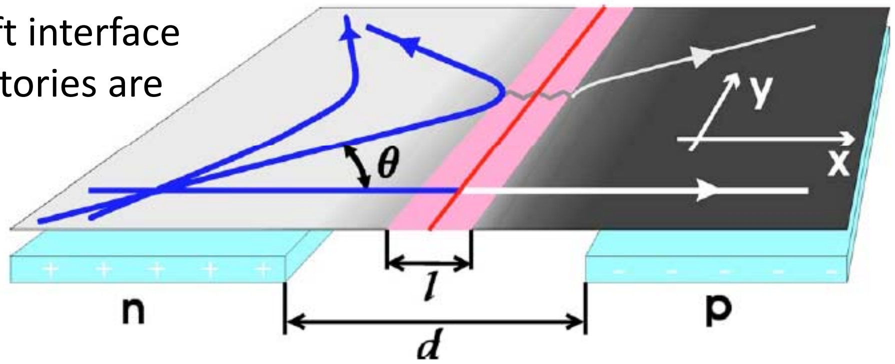

FIG. 1. (Color online) Angular dependence of quasiparticle transmission through the electrostatically generated n-p junction in graphene.

quantum-mechanically the particles can tunnel from one side to the other with probability:

$$w(\theta) = e^{-\pi(k_F d)\sin^2\theta}.$$

Klein effect
Klein tunneling

$$\boxed{G_L = \frac{4e^2}{h}\frac{k_F W}{\pi}\langle T\rangle}$$

where <T> is the mean transmission probability

$$\langle T\rangle = \int_{-\pi/2}^{\pi/2} e^{-\pi k_F d \sin^2(\theta)} \cos(\theta) d\theta$$

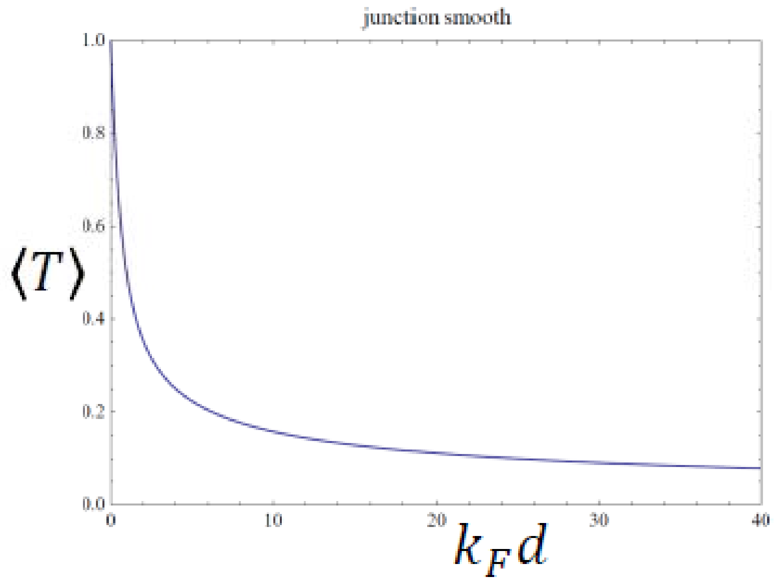

Electron optics in graphene

Graphene
2x2 μm

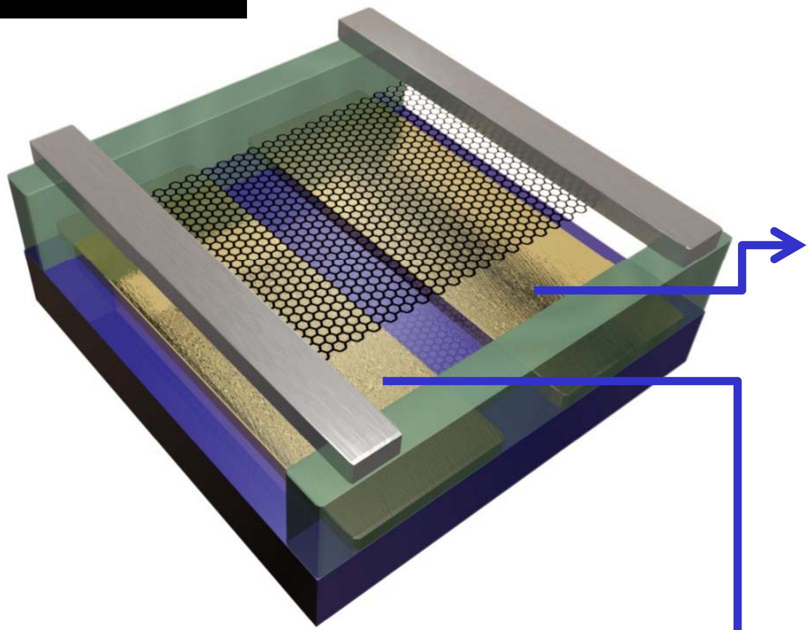

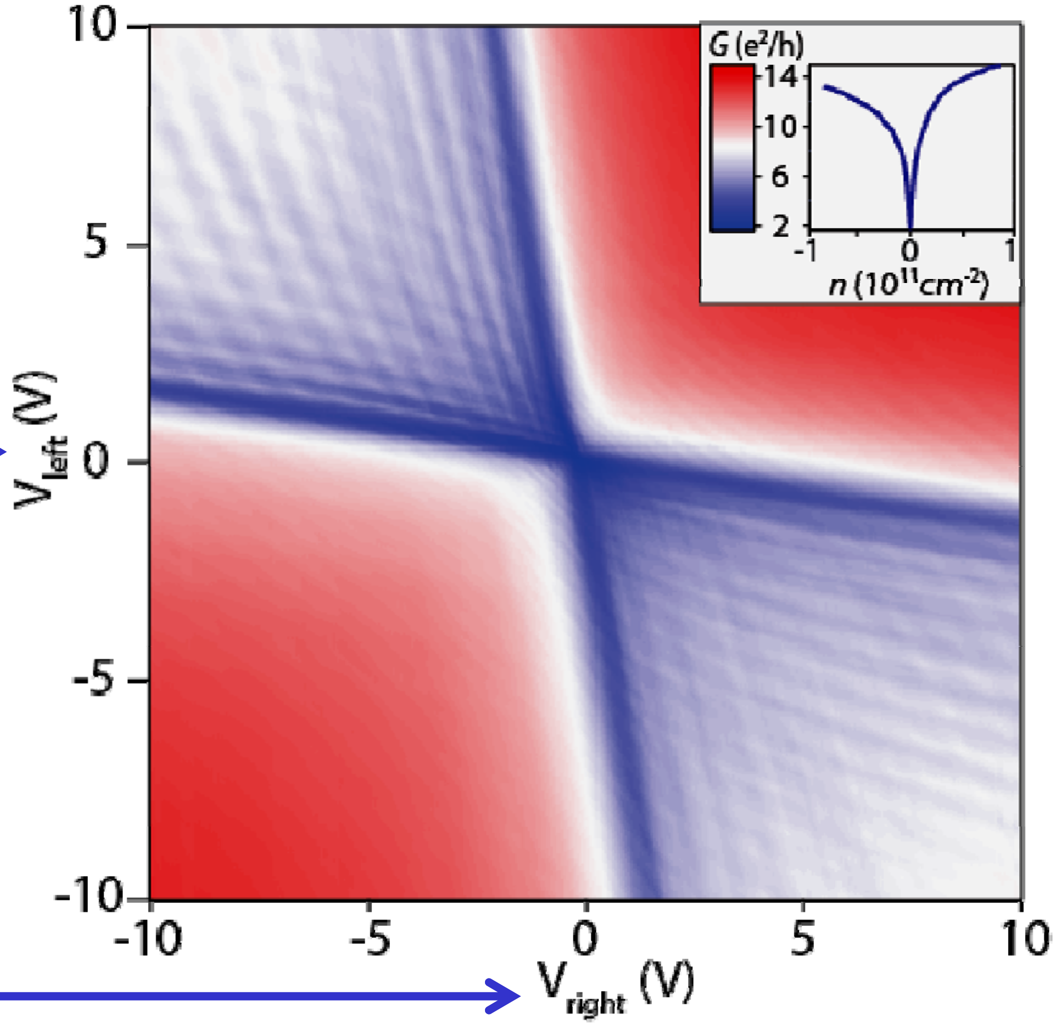

Similar data published in:
P. Rickhaus, R. Maurand, M.H. Liu et al. Nature Comm. 4, 2342 (2013)

Electron optics in graphene

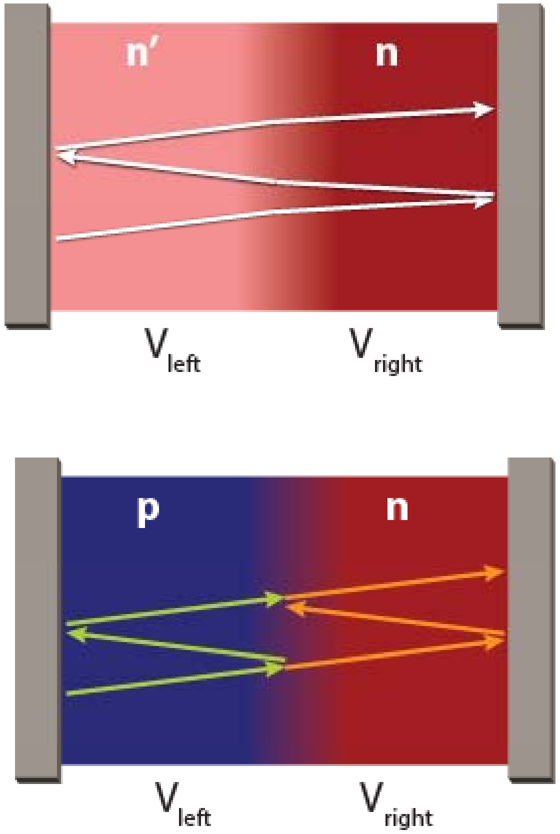

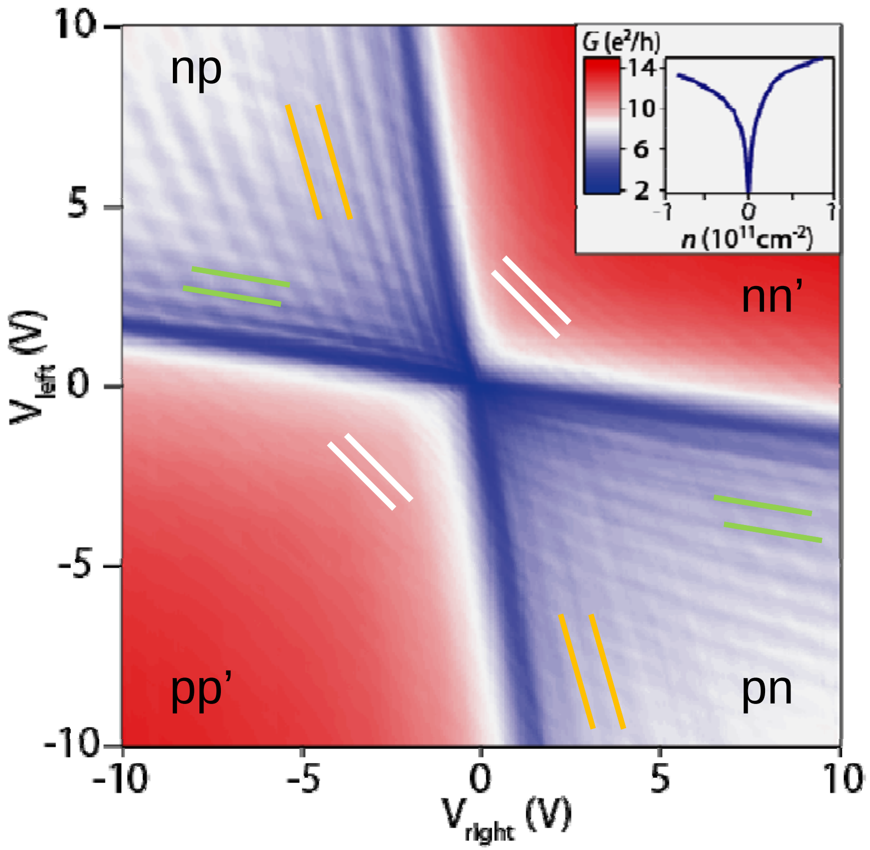

P. Rickhaus, R. Maurand, M.H. Liu et al. Nature Comm. 4, 2342 (2013)

Electron optics in graphene

The Focusing of Electron Flow and a Veselago Lens in Graphene *p-n* Junctions

Vadim V. Cheianov,[1*] Vladimir Fal'ko,[1] B. L. Altshuler[2,3]

The focusing of electric current by a single *p-n* junction in graphene is theoretically predicted. Precise focusing may be achieved by fine-tuning the densities of carriers on the *n-* and *p*-sides of the junction to equal values. This finding may be useful for the engineering of electronic lenses and focused beam splitters using gate-controlled *n-p-n* junctions in graphene-based transistors.

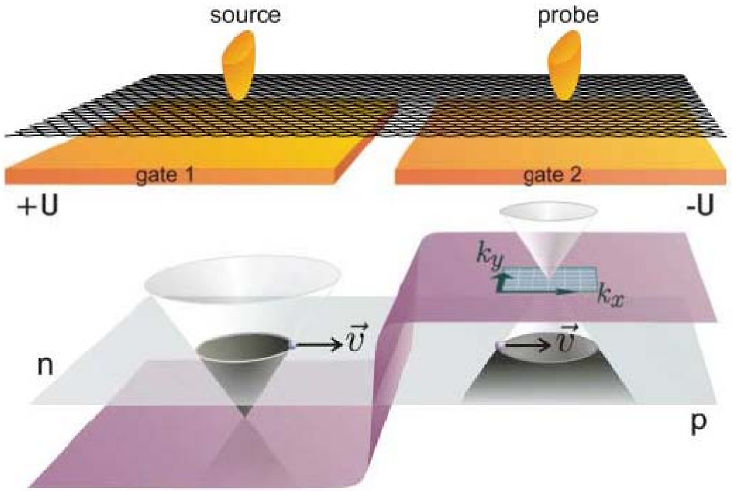

Fig. 1. Graphene *p-n* junction (PNJ). Monolayer of graphite is placed over the split gate, which is used to create *n-* (**left**) and *p*-doped (**right**) regions. The energy diagram shows the position of the Fermi level with respect to the touching point of the valence and the conduction bands.

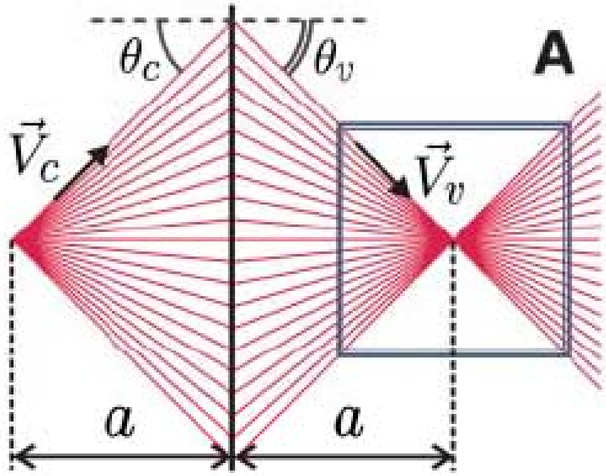

Electron optics in graphene

the real **Klein-tunneling** experiment

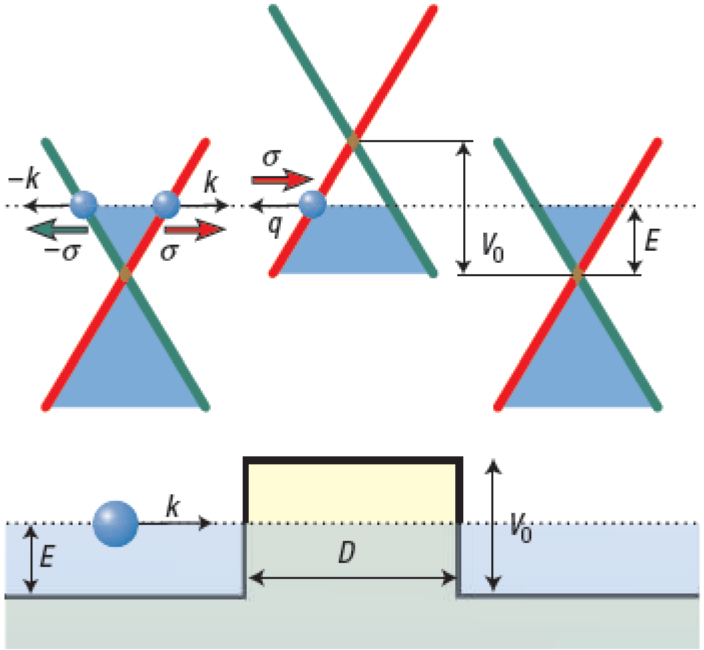

from paper Katsnelson, Novoselov, Geim, Nature. Phys. 2, 620 (2006)

$$\psi_1(x,y) = \begin{cases} (e^{ik_x x} + re^{-ik_x x})e^{ik_y y}, & x < 0, \\ (ae^{iq_x x} + be^{-iq_x x})e^{ik_y y}, & 0 < x < D, \\ te^{ik_x x + ik_y y}, & x > D, \end{cases}$$

$$\psi_2(x,y) = \begin{cases} s(e^{ik_x x + i\phi} - re^{-ik_x x - i\phi})e^{ik_y y}, & x < 0, \\ s'(ae^{iq_x x + i\theta} - be^{-iq_x x - i\theta})e^{ik_y y}, & 0 < x < D, \\ ste^{ik_x x + ik_y y + i\phi}, & x > D, \end{cases}$$

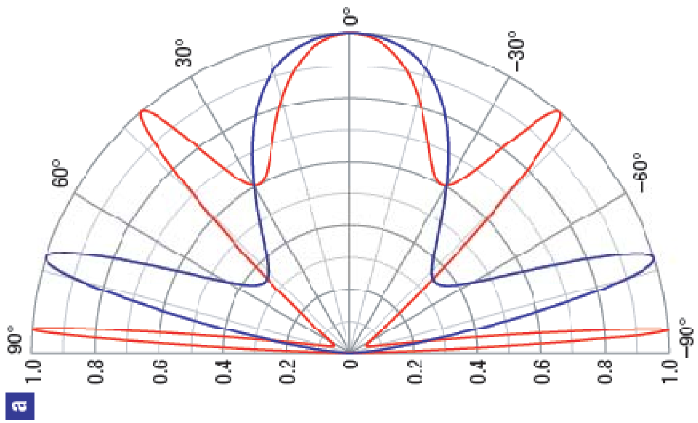

transmission is **always one at normal incidence** in monolayer graphene

7. Pseudodiffusion in graphene

Electron optics in graphene

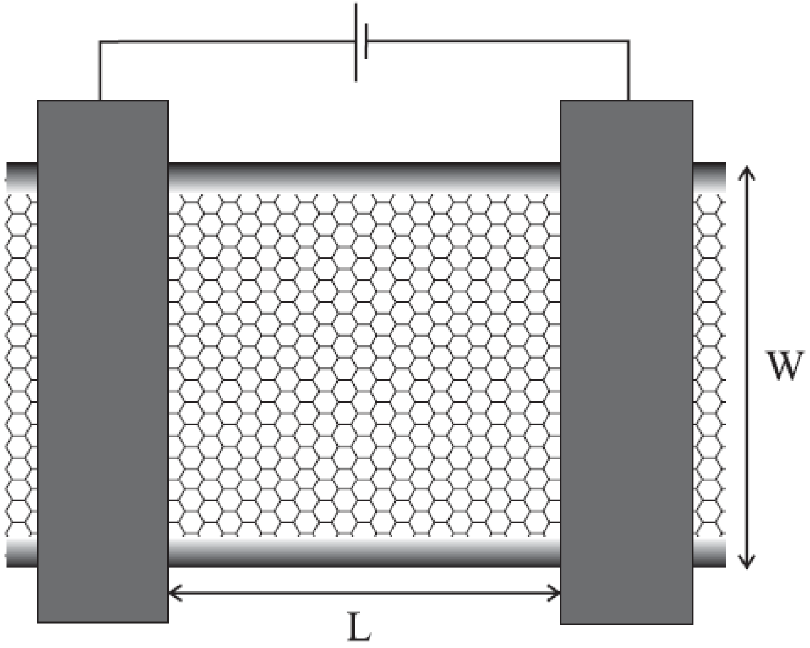

assume all is graphene, also the contacts
but contacts at high doping (very large)

problem is similar to Klein tunneling
matching of wave functions

Tworzydlo et al. Phys. Rev. Lett. 96, 24680 (2006)

Tero Heikkilä's book

$$T(k_y) = \frac{2q_x^2}{2q_x^2 + k_y^2(1-\cos(2q_xL))}, \qquad (10.43)$$

(here, x is along junction, y is transverse. For k_y=0, i.e. normal incidence, transmission probability is 1)

$$G = \frac{2e^2}{h}\sum_n T_n \quad \text{and} \quad F = \frac{\sum_n T_n(1-T_n)}{\sum_n T_n},$$

$$G = \frac{4e^2}{h}\frac{W}{\pi}\int_0^\infty dk_y T(k_y) \qquad G = \frac{4e^2}{\pi h}\frac{W}{L}$$

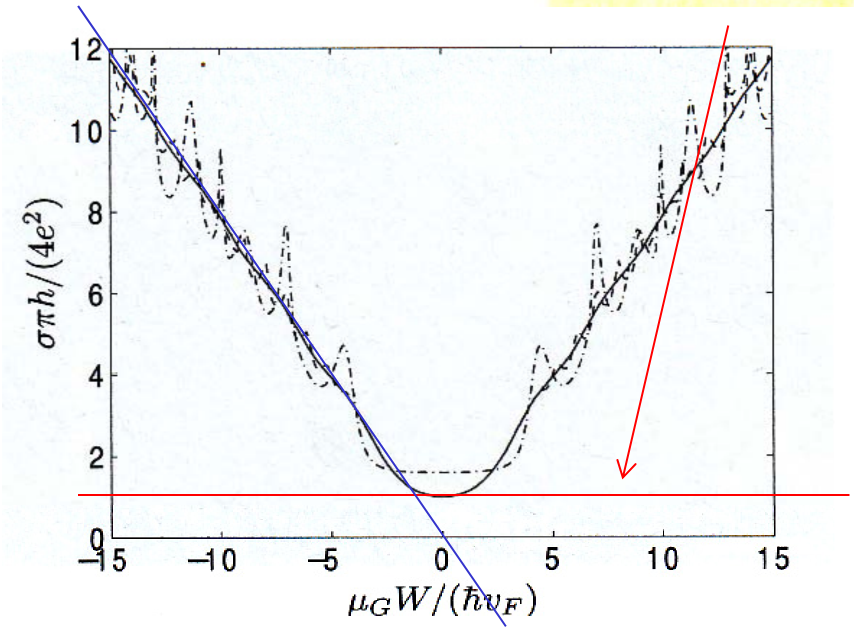

μ_G is chemical potential in graphene

Electron optics in graphene

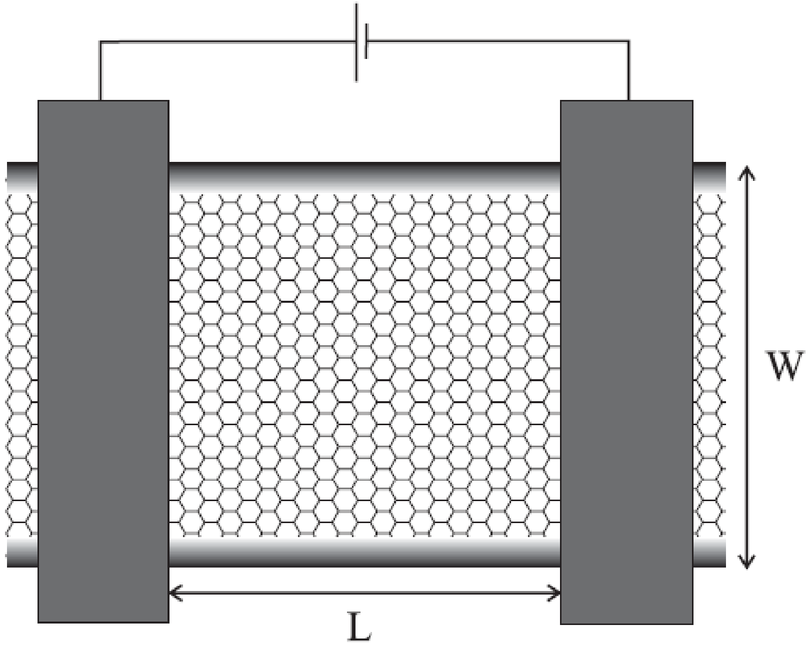

assume all is graphene, also the contacts
but contacts at high doping (very large)

problem is similar to Klein tunneling
matching of wave functions

Tworzydlo et al. Phys. Rev. Lett. 96, 24680 (2006)

Tero Heikkilä's book

$$T(k_y) = \frac{2q_x^2}{2q_x^2 + k_y^2(1-\cos(2q_xL))}, \qquad (10.43)$$

(here, x is along junction, y is transverse. For k_y=0, i.e. normal incidence, transmission probability is 1)

$$G = \frac{2e^2}{h}\sum_n T_n \quad \text{and} \quad F = \frac{\sum_n T_n(1-T_n)}{\sum_n T_n},$$

$$F = \frac{\int_0^\infty dk_y T(k_y)[1-T(k_y)]}{\int_0^\infty dk_y T(k_y)}$$

F=1/3 at the CNP !!

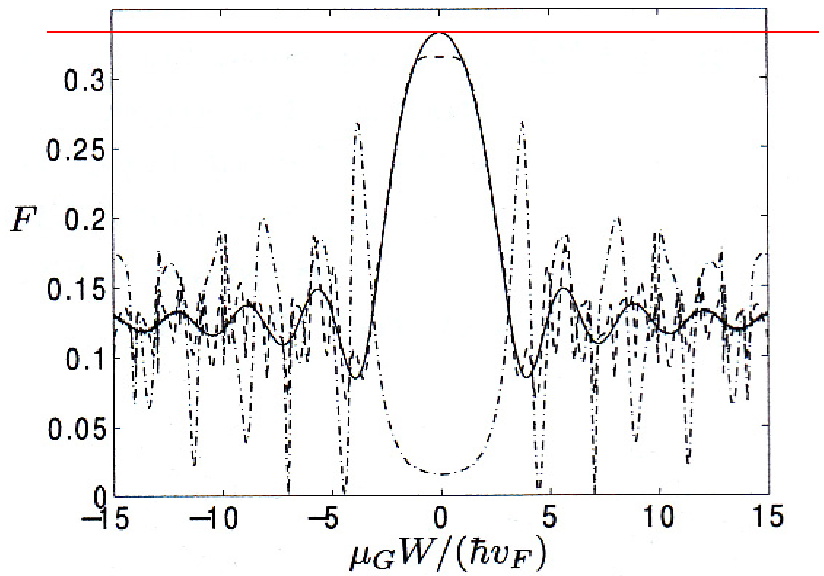

μ_G is chemical potential in graphene

Electron optics in graphene

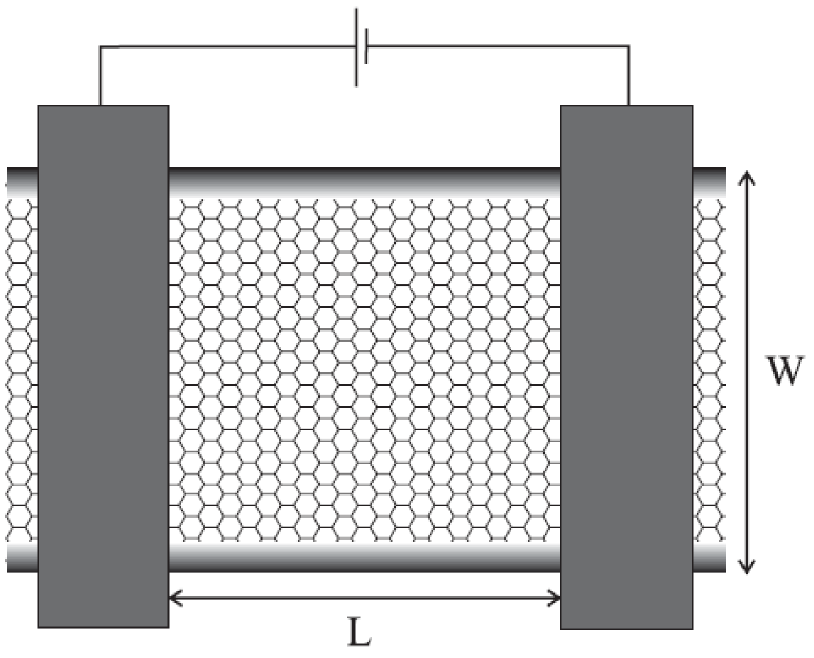

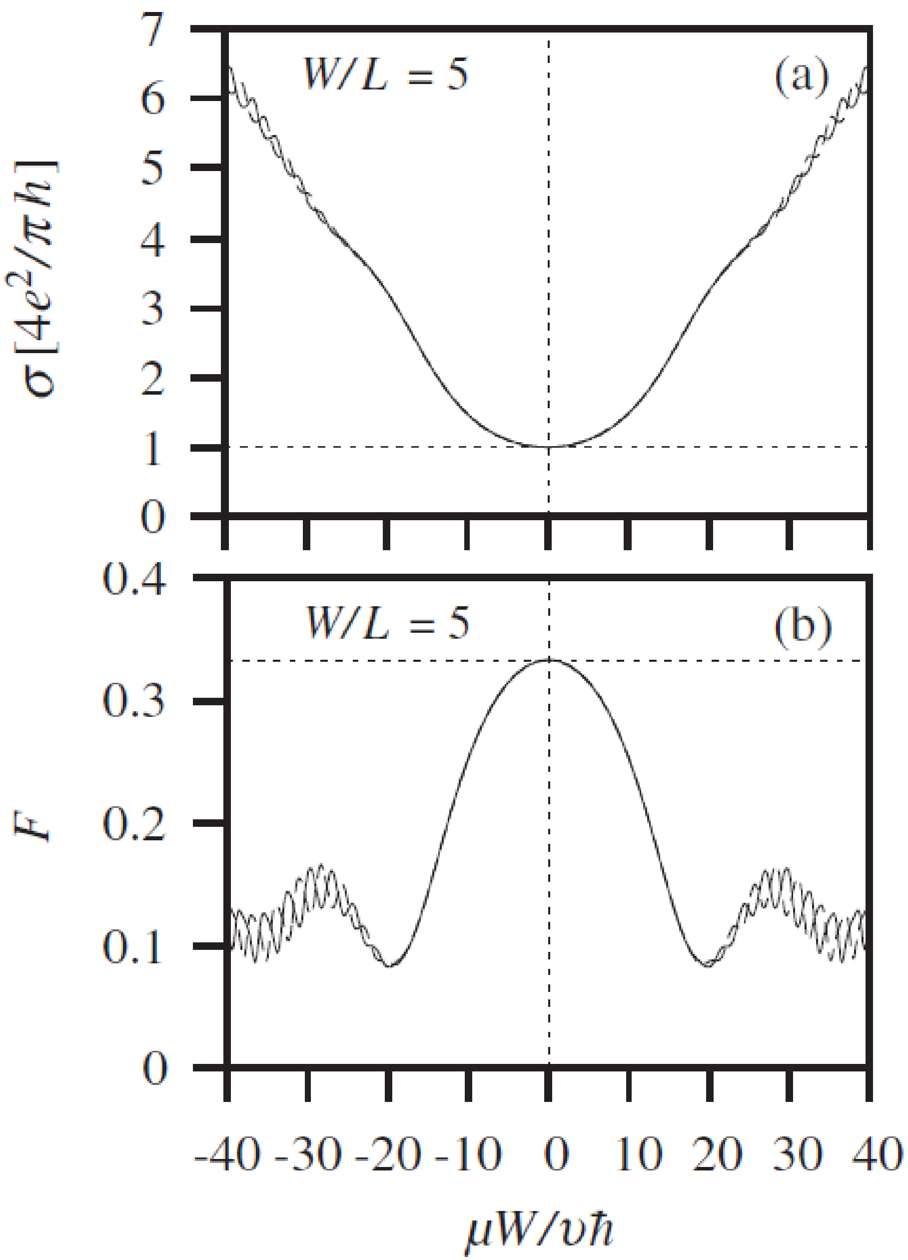

assume all is graphene, also the contacts
but contacts at high doping (very large)

problem is similar to Klein tunneling
matching of wave functions

Tworzydlo et al. Phys. Rev. Lett. 96, 24680 (2006)

“pseudo-diffusion in graphene”

PRL **100,** 156801 (2008) PHYSICAL REVIEW LETTERS week ending 18 APRIL 2008

Shot Noise in Graphene

L. DiCarlo,[1] J. R. Williams,[2] Yiming Zhang,[1] D. T. McClure,[1] and C. M. Marcus[1]
[1]*Department of Physics, Harvard University, Cambridge, Massachusetts 02138, USA*
[2]*School of Engineering and Applied Sciences, Harvard University, Cambridge, Massachusetts 02138, USA*
(Received 20 November 2007; published 14 April 2008)

We report measurements of current noise in single-layer and multilayer graphene devices. In four single-layer devices, including a *p-n* junction, the Fano factor remains constant to within ±10% upon varying carrier type and density, and averages between 0.35 and 0.38. The Fano factor in a multilayer device is found to decrease from a maximal value of 0.33 at the charge-neutrality point to 0.25 at high carrier density. These results are compared to theories for shot noise in ballistic and disordered graphene.

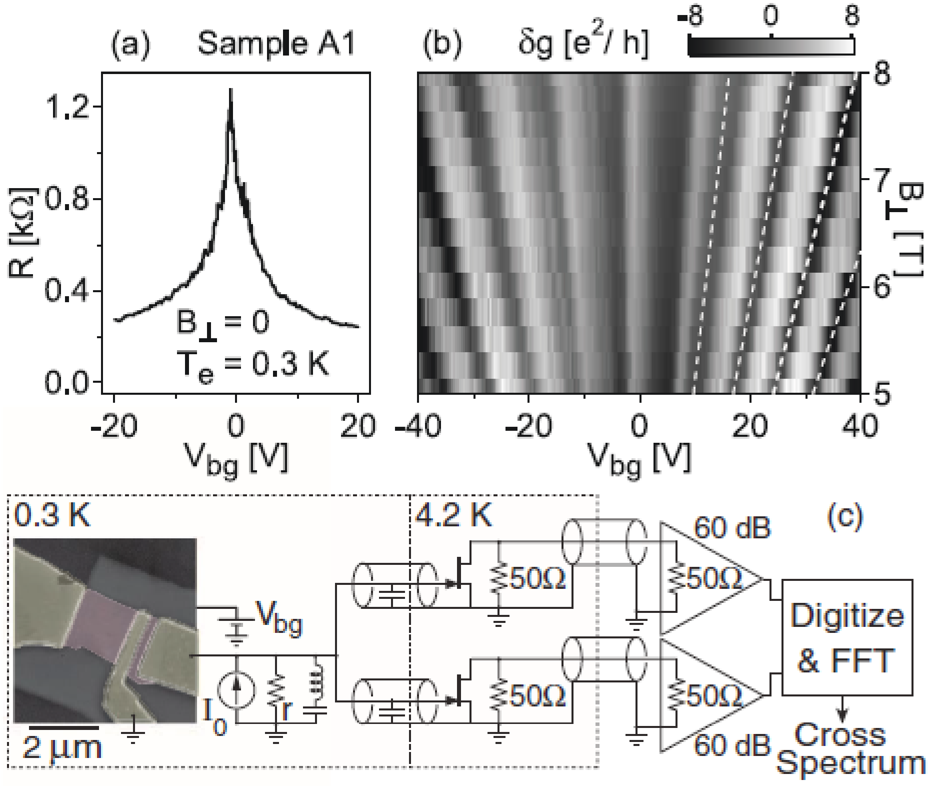

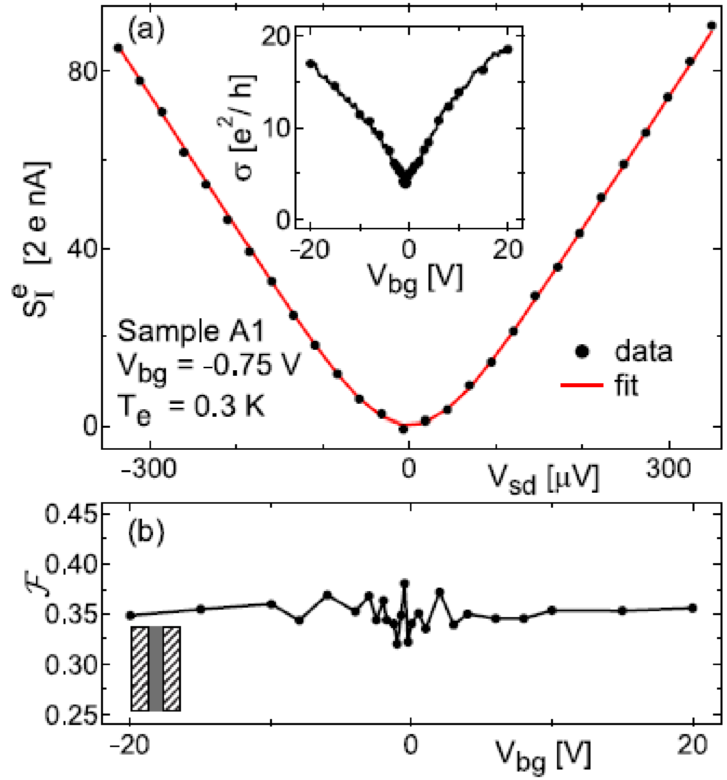

"pseudo-diffusion in graphene"

PRL **100,** 196802 (2008) PHYSICAL REVIEW LETTERS week ending 16 MAY 2008

Shot Noise in Ballistic Graphene

R. Danneau,[1,*] F. Wu,[1] M. F. Craciun,[2] S. Russo,[2] M. Y. Tomi,[1] J. Salmilehto,[1] A. F. Morpurgo,[2] and P. J. Hakonen[1]
[1]*Low Temperature Laboratory, Helsinki University of Technology, Espoo, Finland*
[2]*Kavli Institute of Nanoscience, Delft University of Techn*

(Received 27 November 2007; published

We have investigated shot noise in graphene field effect devices low frequency (f = 600–850 MHz). We find that for our graphene ratio W/L, the Fano factor $\mathfrak{F}$ reaches a maximum $\mathfrak{F} \sim 1/3$ at the D with increasing charge density. For smaller W/L, the Fano factor a results are in good agreement with the theory describing that transp arises from evanescent electronic states.

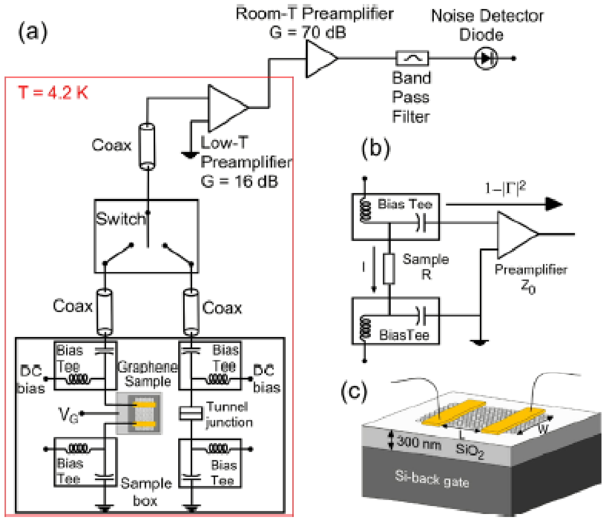

FIG. 1 (color online). (a) Experimental setup for detecting shot noise at T = 4.2–30 K. (b) Schematic of the principle of our measurements in terms of the noise power reflection $|\Gamma|^2$. (c) Illustration of a typical graphene sample fabricated for our shot noise study.

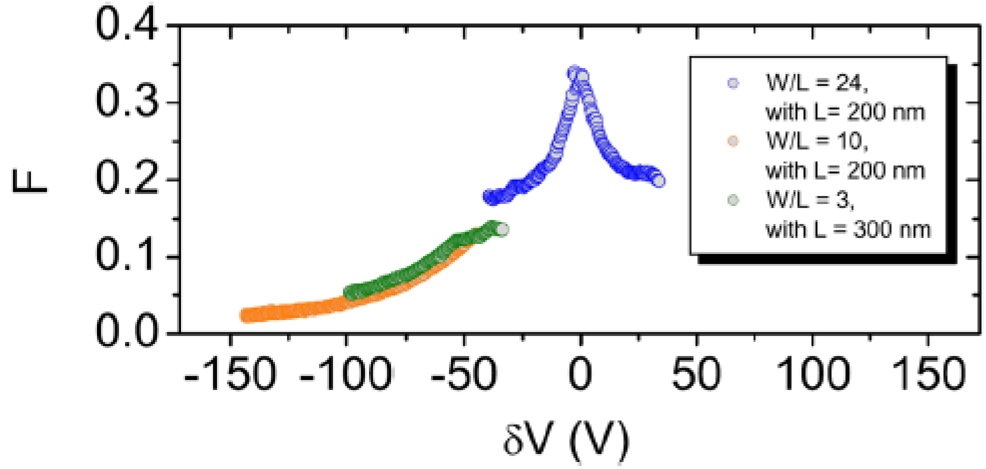

FIG. 3 (color online). F extracted at V_{bias} = 40 mV for three different samples, all having $W/L \geq 3$, as a function of $\delta V = V_{\mathrm{gate}} - V_{\mathrm{Dirac}}$. For the two unintentionally highly p-doped samples (orange and green dots), the Dirac point was estimated via extrapolation of the minimum conductivity at $\frac{4e^2}{\pi h}$.

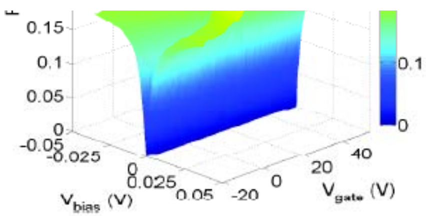

9. Outlook

Transparent electrodes

Production of a 100-m-long high-quality graphene transparent conductive film by roll-to-roll chemical vapor deposition and transfer process

Toshiyuki Kobayashi,[a] Masashi Bando, Nozomi Kimura, Keisuke Shimizu, Koji Kadono, Nobuhiko Umezu, Kazuhiko Miyahara, Shinji Hayazaki, Sae Nagai, Yukiko Mizuguchi, Yosuke Murakami, and Daisuke Hobara
Advanced Materials Laboratories, Sony Corporation, Atsugi-Shi, Kanagawa 243-0014, Japan

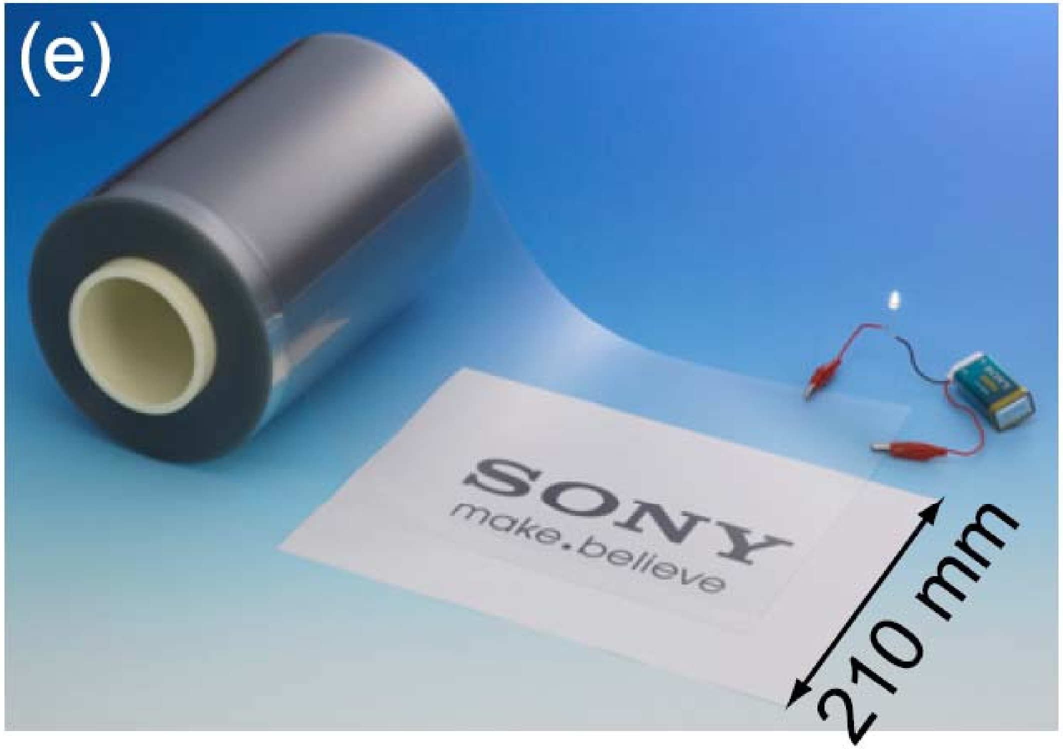

100 Meter lang !

Transparent electrodes

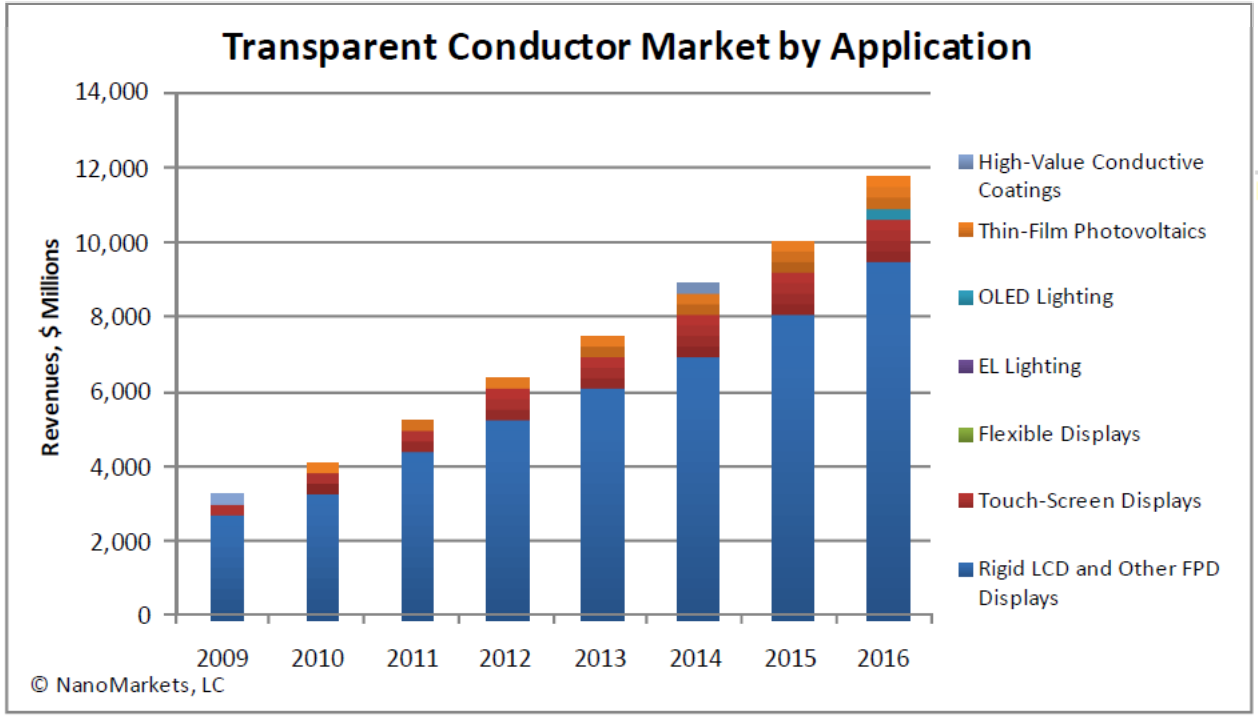

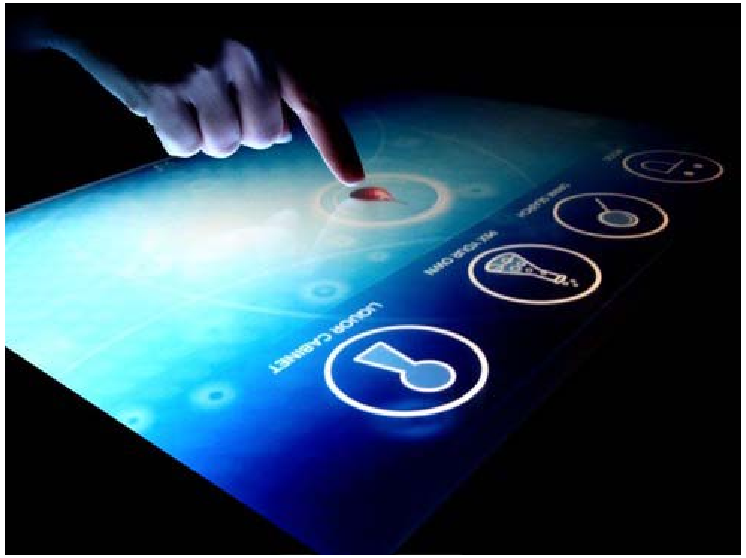

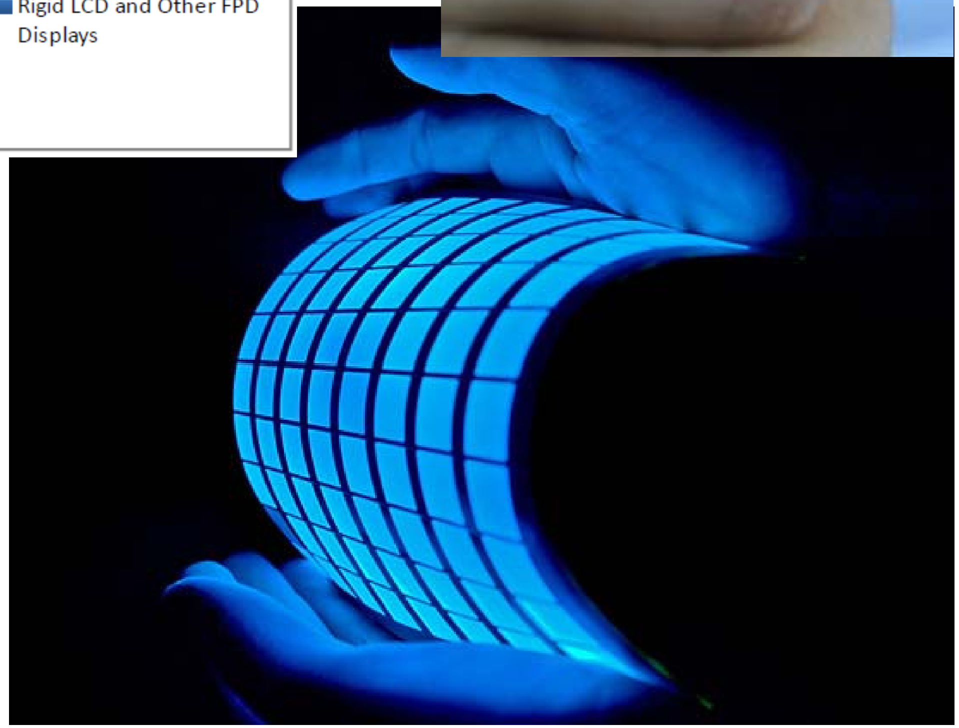

Flexibility...

Mechanically strong

- Reißfestigkeit σ_A = 42 N m^{-1} (**>> σ_A (Stahl)** = 0.084 – 0.4 N m^{-1} für Graphendicke)

  => Trägt 4 kg (z.B. Katze)

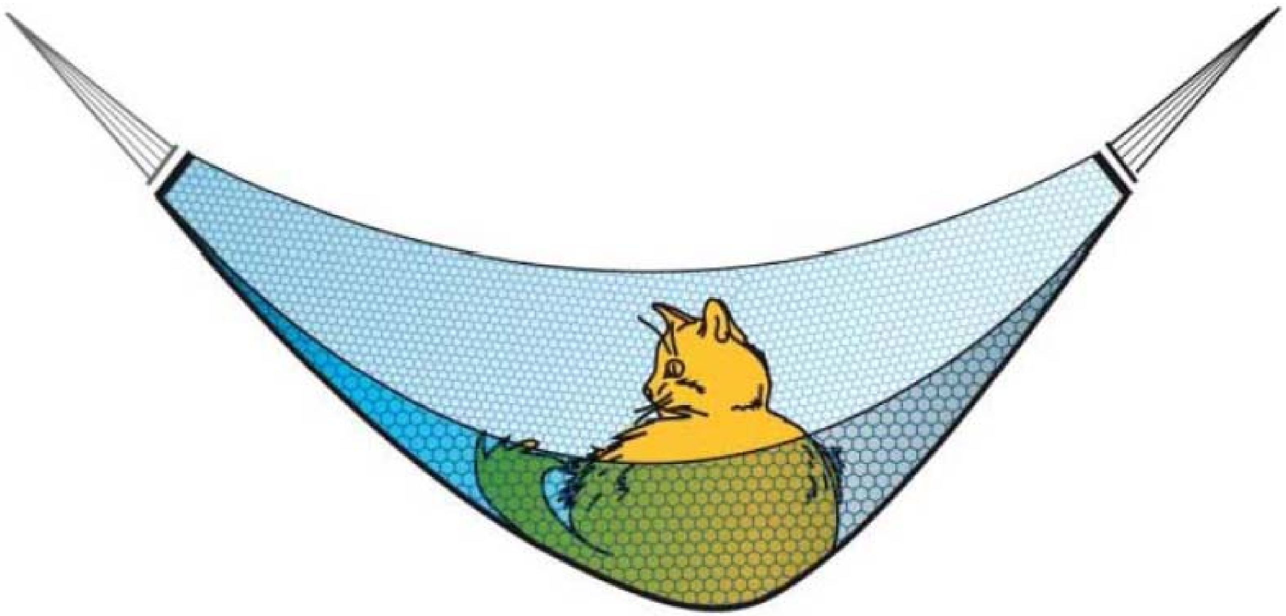

- **Perfekte Barriere** für Gase und Flüssigkeiten

Mechanically strong

?

Stretchability of graphene

Measurement of the Elastic Properties and Intrinsic Strength of Monolayer Graphene

SCIENCE VOL 321 18 JULY 2008

Changgu Lee,[1,2] Xiaoding Wei,[1] Jeffrey W. Kysar,[1,3] James Hone[1,2,4]*

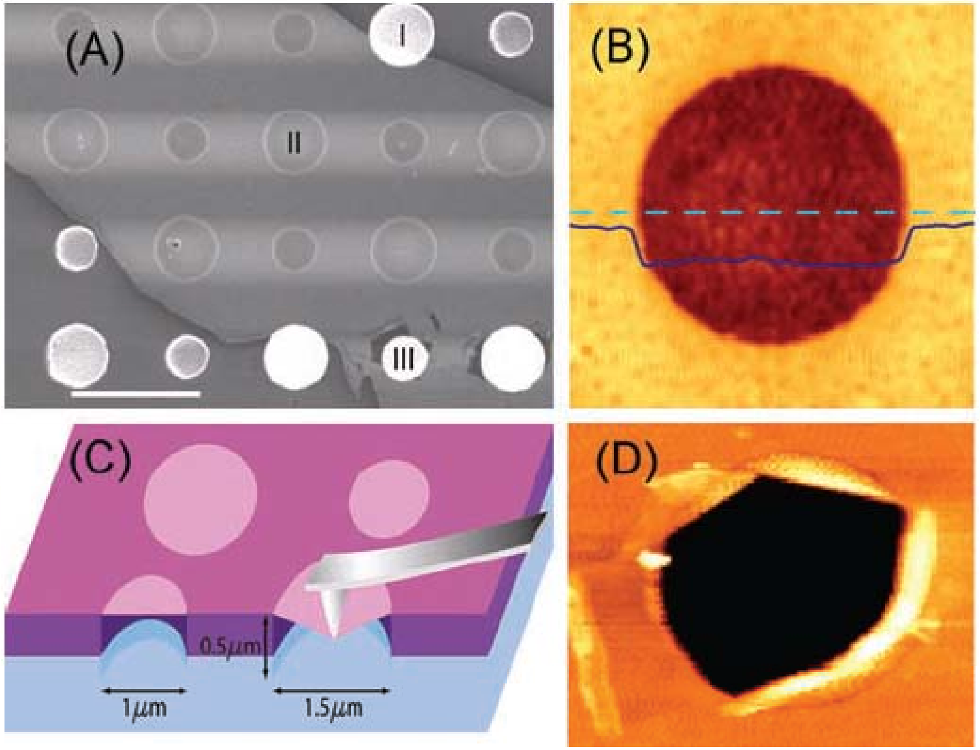

Fig. 1. Images of suspended graphene membranes. (**A**) Scanning electron micrograph of a large graphene flake spanning an array of circular holes 1 μm and 1.5 μm in diameter. Area I shows a hole partially covered by graphene, area II is fully covered, and area III is fractured from indentation. Scale bar, 3 μm. (**B**) Noncontact mode AFM image of one membrane, 1.5 μm in diameter. The solid blue line is a height profile along the dashed line. The step height at the edge of the membrane is about 2.5 nm. (**C**) Schematic of nanoindentation on suspended graphene membrane. (**D**) AFM image of a fractured membrane.

25% möglich
gewöhnliche Materialien
liegen bei 1%

dabei ca. 120 Gpa
mehr als 10 x besser
als Stahl !

Anwendung
Dehnsensor!

Mechanically strong

Graphene used to create more pleasurable condoms

Nobel Prize winning super-material graphene is being used to create thinner and stronger condoms that could be more pleasurable to use

Ein neues Wundermaterial für Kondome, Graphene, möchte der Microsoft-Gründer und reichste Mensch der Welt, Bill Gates, im Kampf der Bill and Melinda Gates Foundation gegen die weltweite Ausbreitung von HIV und AIDS, aber auch Armut, wissenschaftlich weiter entwickeln lassen und zwar am National Graphene Institute Manchester in Großbritannien. Bis 2015 sollen die neuen Kondome an den Start kommen.

Bill Gates will bessere Graphene Kondome statt Latex Kondome für die Welt

21.11.2013 , mehr zum Thema Tests

Graphene is impermeable

Impermeable Atomic Membranes from Graphene Sheets

J. Scott Bunch, Scott S. Verbridge, Jonathan S. Alden, Arend M. van der Zande, Jeevak M. Parpia, Harold G. Craighead, and Paul L. McEuen*

NANO LETTERS
2008
Vol. 8, No. 8
2458-2462

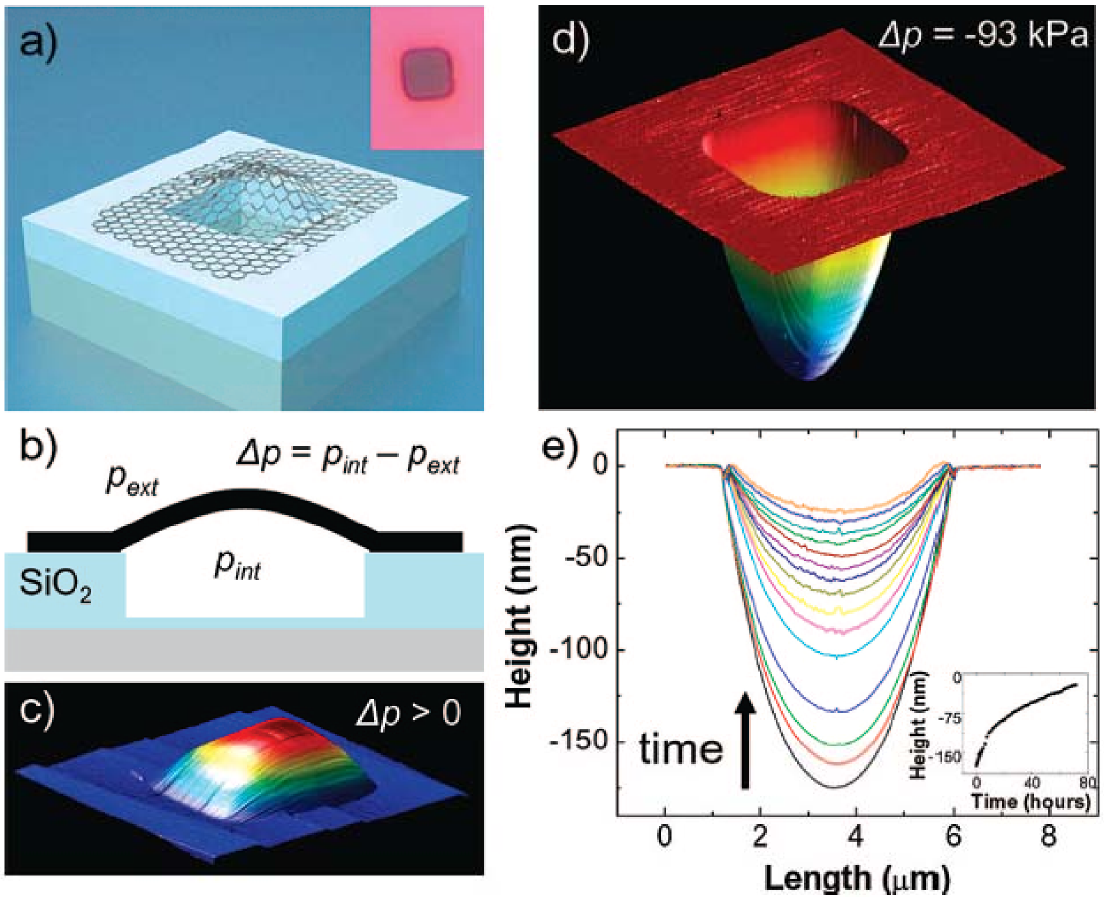

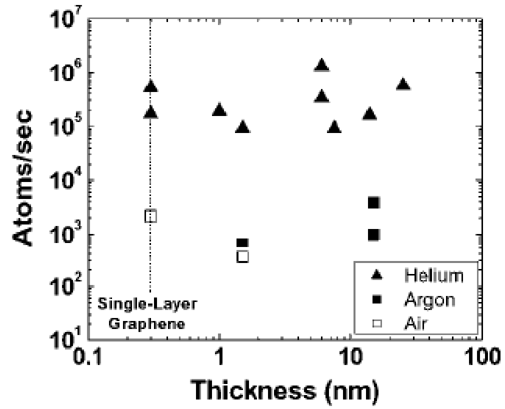

Figure 2. Scatter plot of the gas leak rates vs thickness for all the devices measured. Helium rates are shown as solid triangles (▲), argon rates are shown as solid squares (■) and air rates are shown as hollow squares (□).

Anwendungen: einstellbarer mechanischer Schwingkreis
Drucksensor
Gasdichtung
Nanobehältnis für Medikamente

Graphene electronics

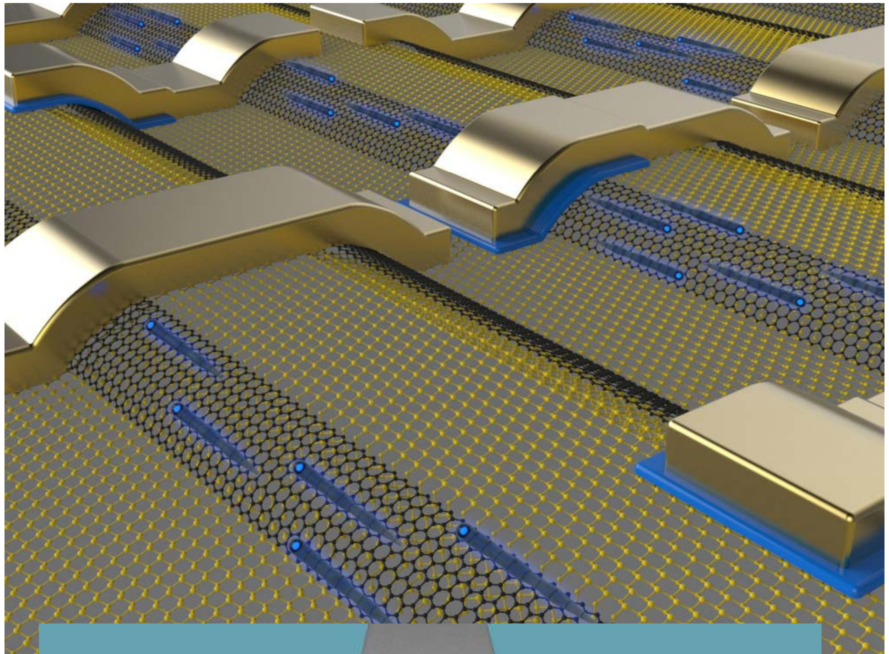

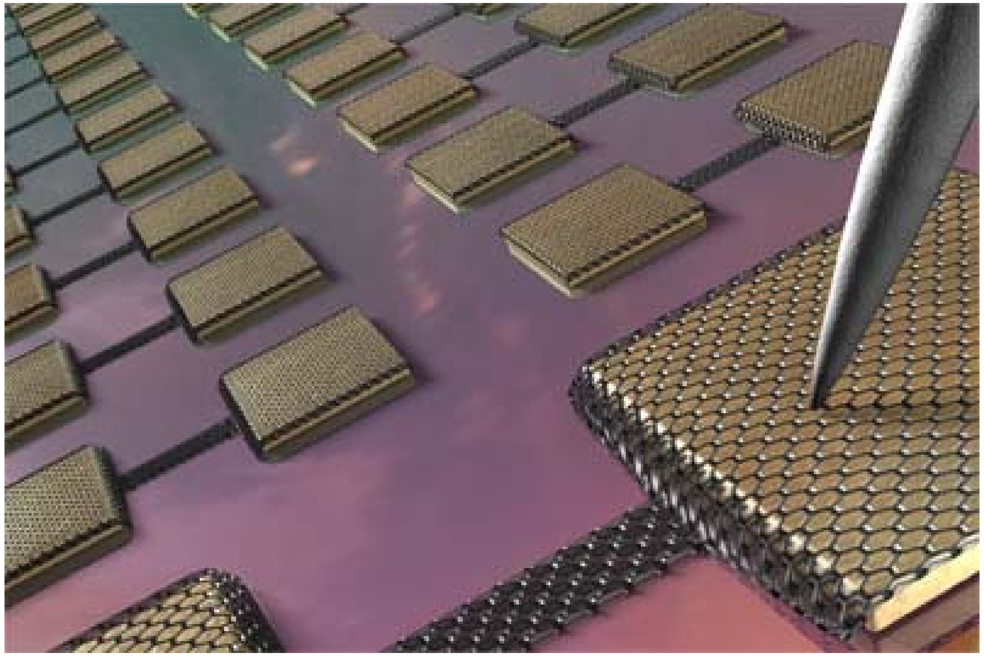

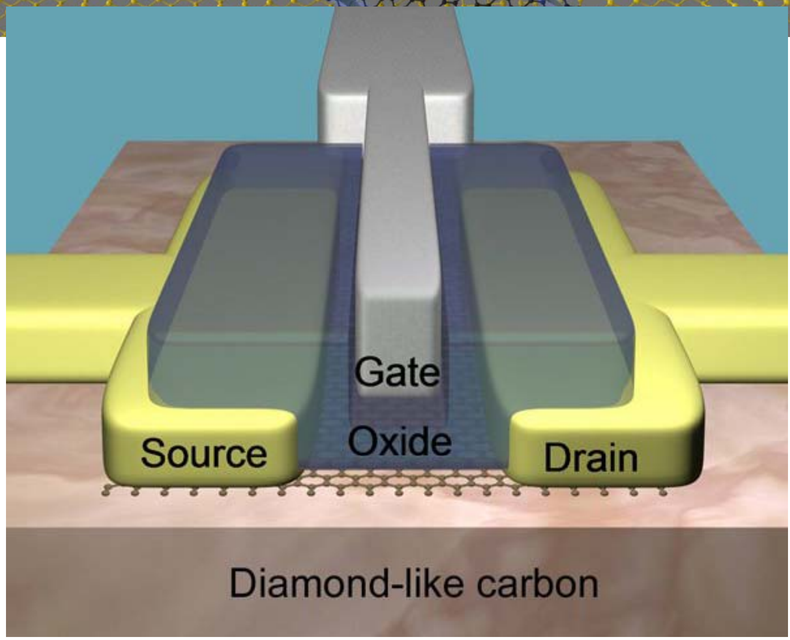

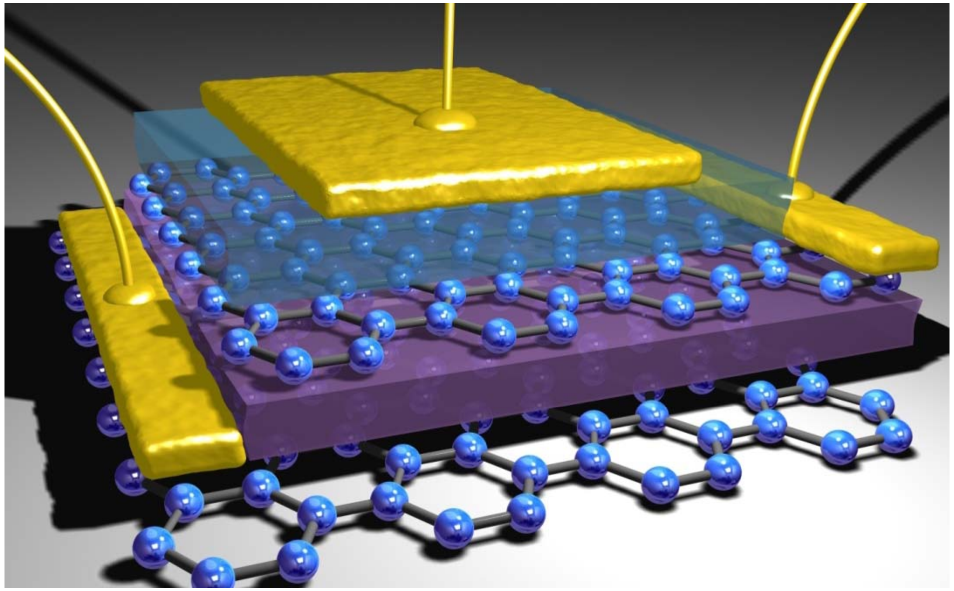

Dehnsensor aus Graphen

Graphene-based transparent strain sensor

CARBON 51 (2013) 236–242

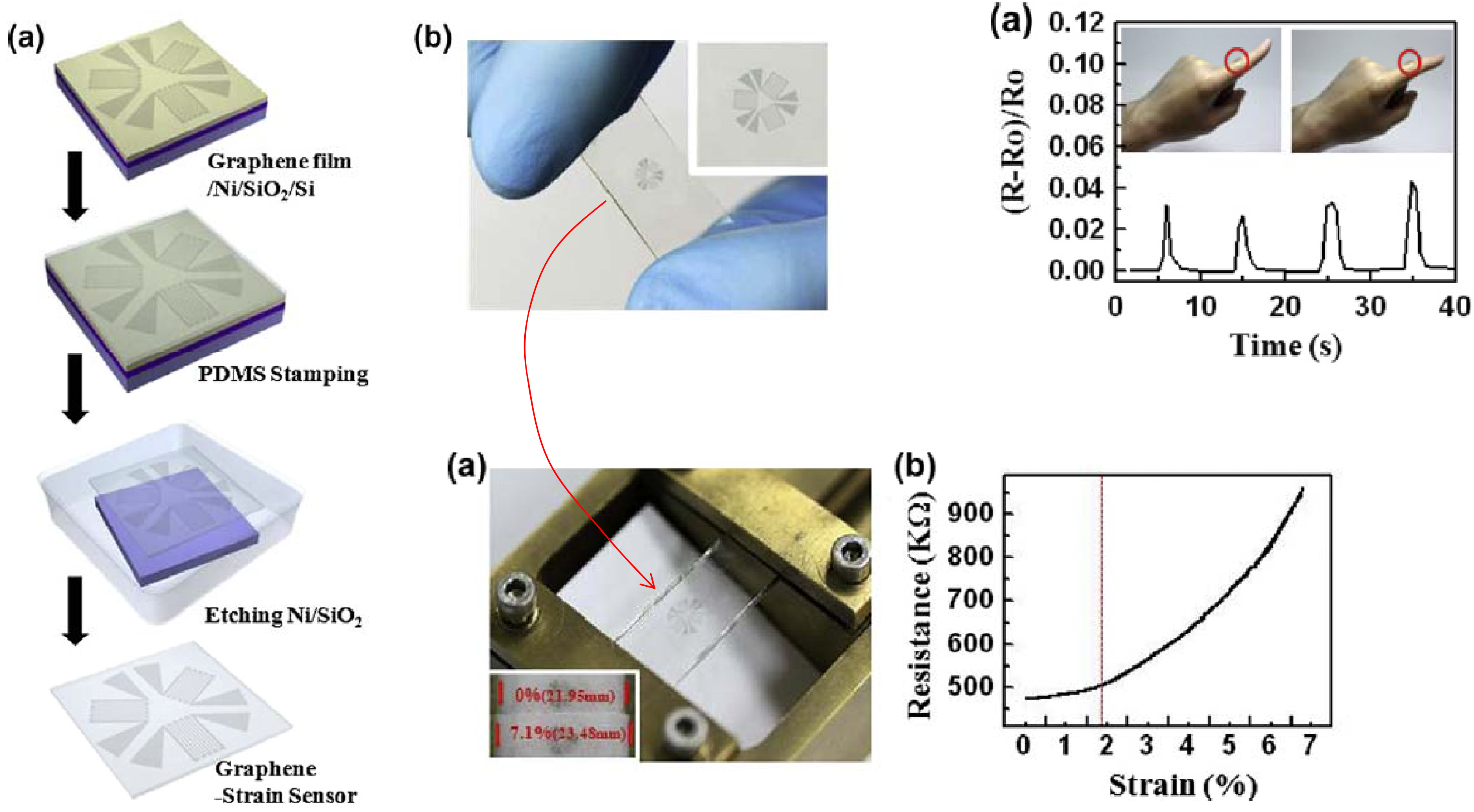

Other 2D materials

BN = Isolator

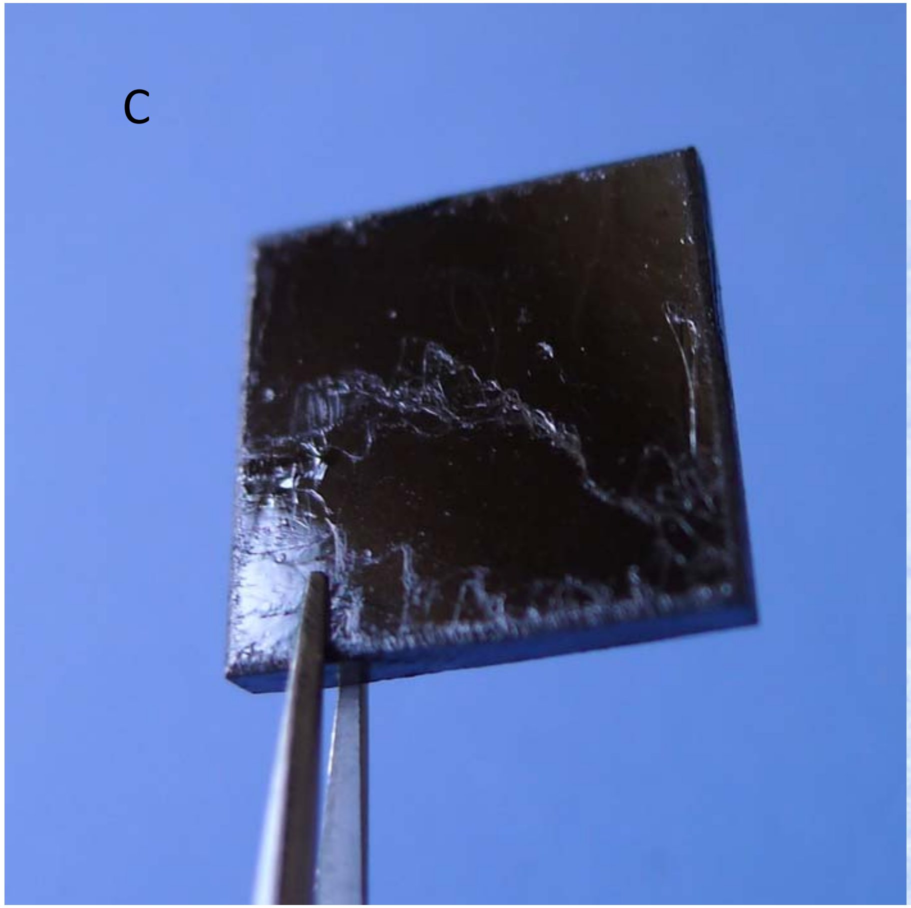

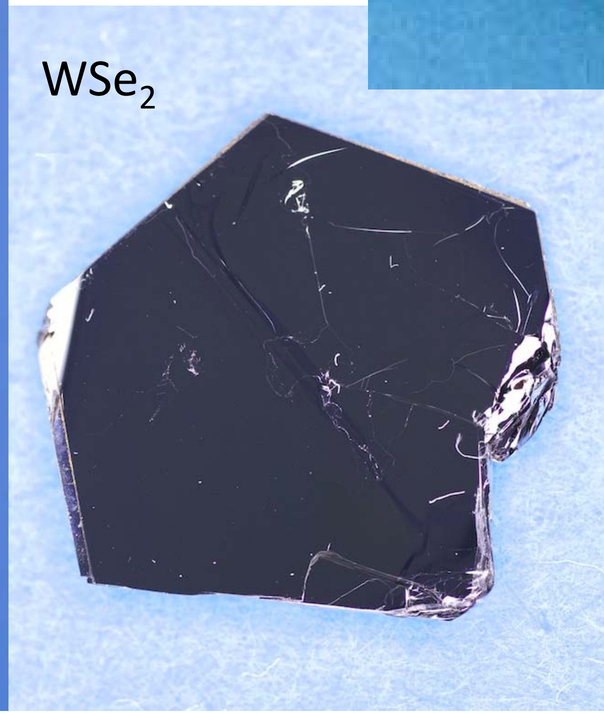

guiding

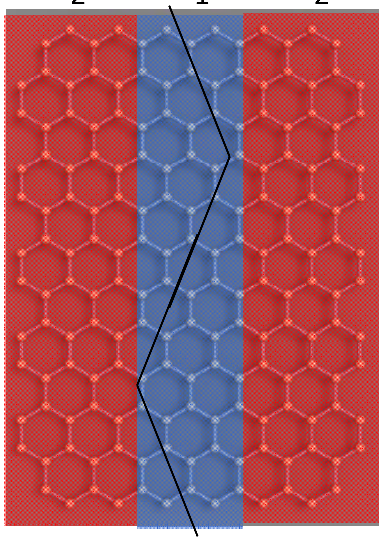

$$n' = \pm k_F = \sqrt{\pi |n|}$$

$$n_1' \sin(\alpha_1) = n_2' \sin(\alpha_2)$$

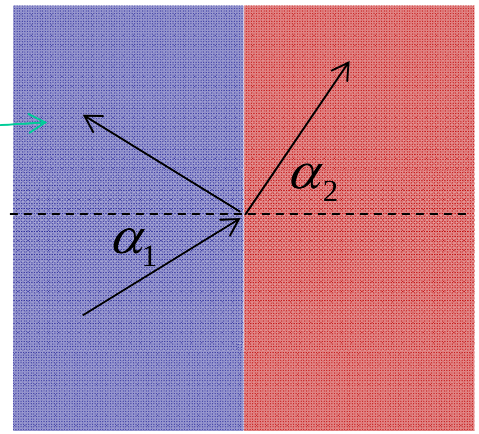

total internal reflection if:

$$n_1' \sin(\alpha_1) > n_2'$$

two cases: **conventional optical guiding** (refractive indicies have the same sign) and **pn-guiding** *Williams, et al. Nature Nano* ***6****, 222–5 (2011).*